UTRECHT UNIVERSITY - FACULTY OF GEOSCIENCES

DESIGNING A LOCAL CARBON NEUTRAL ENERGY SYSTEM VIA MULTI ENERGY SYSTEM OPTIMISATION

A case study of Utrecht University

Babette Korevaar
Student number: 3992039
E-mail: b.korevaar@students.uu.nl

Utrecht University

Superviser: Dr. Matteo Gazzani
Co-superviser: Lukas Weimann
Master's thesis Energy Science (GEO4-2510)
Utrecht, The Netherlands
October 2019

Abstract

In the Energy Agenda of the Province of Utrecht, Utrecht Science Park is designated as experimental area for sustainable energy, which aims to develop a self-sufficient energy supply system. Utrecht University, owner of Utrecht Science Park, wants to accelerate the energy transition and therefore has the ambition to be carbon neutral by 2030. Currently, the system operates for a small share on renewable energy technologies. This study examines two scenarios for a self-sufficient energy system compliant with the goal of 2030; at which (I) Utrecht University operates as end user of electricity and (II) Utrecht University operates as end user of electricity and heat. These two scenarios contain multiple sub-scenarios, for which optimisation designs are modelled through Mixed Integer Linear Programming (MILP). Key findings of the performed energy system optimisations for the different scenarios are; scenario (I) full decarbonisation could be achieved, while for scenario (II) this was unfeasible. In this process an existing MILP tool for multi energy system optimisation is used. The designs are optimised in terms of total annual costs and CO_2 emissions. Along the Pareto front the optimised designs are evaluated on cost, technology sizes and storage distribution. Subsequently, the need for seasonal storage and the most favourable renewable energy technologies for a decarbonised energy system is examined. An additional analysis is performed to indicate under which circumstances Utrecht University should contribute to the geothermal project which is currently in research phase. Finally, the sensitivity of the systems costs is analysed.

Keywords: MILP, multi energy system optimisation, decarbonisation, Utrecht University, self-sufficient, renewable energy technologies, energy transition, carbon neutral, E-Hub

Acknowledgements

I would like to thank Matteo Gazzani for his expertise and encouragement throughout this research, as well as Lukas Weimann for his help in understanding the E-Hub tool and his support during the whole process. Having the weekly Energy Team meetings kept me on the right track and was an inspiring and educational but above all extremely valuable way to receive feedback. I really appreciate that they have both spent their precious time on supporting my research. Lastly I would like to thank Frans Tak for his effort in obtaining the data of Utrecht University and providing me with information about the current energy system. I hope that this research can give a valuable contribution to the Energy Team of Utrecht University to achieve full decarbonisation of their energy supply.

Babette Korevaar
Utrecht, October 2019

Contents

1 Introduction **1**

1.1 Research questions . . . 2
1.2 Relevance of the research . . . 3
1.3 Outline . . . 3

2 Theoretical Background **4**

2.1 Multi Energy Systems . . . 4
2.2 Key technologies . . . 4
2.2.1 Conversion technologies . . . 4
2.2.2 Storage Systems . . . 6

3 Methodology **7**

3.1 The E-Hub . . . 7
3.2 System Description and optimisation problem . . . 8
3.2.1 Objective function . . . 8
3.3 Mixed Integer Linear Programming . . . 10
3.3.1 Branch and Bound . . . 10
3.3.2 Multi objective approach . . . 11
3.4 Input data . . . 12
3.4.1 Weather data . . . 12
3.4.2 Current installations . . . 13
3.4.3 Spatial limitations renewables . . . 13
3.4.4 Demand . . . 15
3.5 Case Studies . . . 24

4 Results I - Electricity supply **26**

4.1 Levels of decarbonisation . . . 27
4.1.1 Invest to decarbonise . . . 27
4.1.2 Technology sizes . . . 28
4.1.3 Technology outputs . . . 29
4.1.4 Storage . . . 30
4.2 Introducing Power To Gas . . . 32

4.2.1 Effect of introduction of PtG on the cost and size of technologies 32
4.2.2 Cost and size influence due Power to Gas 32
4.2.3 Storage distribution 35

5 Results II - Electricity and heat supply **36**
5.1 Multi energy system approach 37
5.1.1 Feasibility of local generation of heat and electricity 37
5.1.2 Technology sizes 38
5.1.3 Storage distribution 39
5.2 Introducing Geothermal heat 43
5.2.1 Impacts on the configuration and operation of the system 43
5.2.2 Geothermal heat versus green gas 46
5.2.3 Emission free geothermal heat 47

6 Sensitivity of system costs **50**
6.1 Solar area 50
6.2 Energy prices 50
6.3 Energy demand 51

7 Discussion **53**

8 Conclusion **56**

A Utrecht University Campus **62**
A.1 Campus map 63
A.2 Energy use Utrecht University 2018 64
A.3 Energy networks Campus 65
A.3.1 Heat network connections 66
A.3.2 ATES connections 67

B Technologies **68**
B.1 Input data for conversion and storage technologies 69
B.2 Cost coefficients of conversion and storage technologies. 69

List of Figures

3.1 Schematic representation of the investigated system supplying heat and electricity to the end user Utrecht University. Green lines represent electricity transfer, yellow solar irradiance, blue wind energy, red heat, grey natural gas and purple hydrogen. The available set of technologies in the E-Hub relevant to analysis for UU are PV panels, ST, WTs, HWTS, PtG, HOS, LiBs, edHPs. Existing PV panels and ATES systems are excluded as technologies in the optimised systems, since the operation of the two technologies are processed in the demand. 8

3.2 Weather data of weather station De Bilt with an hourly frequency of 2018, with (a) the solar irradiance in $\mathrm{kW\,h\,m^{-2}}$, (b) the wind speed in $\mathrm{m\,s^{-1}}$ and (c) the ambient temperature in °C. 12

3.3 Aerial view of Utrecht Science Park with the locations of the currently suitable solar fields, parking lots and solar roofs. The fields are marked in green, parkings in blue and roofs in yellow. The red area represents the unsuitable area solar fields. 15

3.4 The PV production by the existing PV panels is presented with an hourly time interval of 2018. The electricity is produced by 4600 PV panels which are located at roofs of UU buildings. The peak performance of the installed PV panels is 1.2 MW_p. 17

3.5 The expected electrical demand of UU with an hourly time interval of 2018. The electricity profile is the sum of the demand of UU buildings minus the generated electricity of the existing PV panels installed at UU. 17

3.6 Heat demand 10 buildings with an hourly time interval of year 2018, with (a) *01.12 Bleekergeb. (Sorbonnelaan 4)*, (b) *01.23 Ornsteinlab. (Princetonplein 1)*, (c) *01.35 NITG-TNO (Princetonlaan 6)*, (d) *01.52 Buys Ballot lab. (Princetonpl. 5)*, (e) *01.58 Aardwetenschappen (Budapestlaan 4)*, *(f) 02.28 Res.kas+Bot.tuin (Uppsalaln Tuin)*, (g)*02.60 D.de Wiedgeb (Universiteitswg 99)*, (h) *03.77 Hugo Kruytgebouw (Padualaan 8)* (i) *05.27 Univers.Bibliot (Heidelberglaan 3)* and (j) *13.22 Androclusgebouw (Yaleln 1)*. 19

3.7 Generic heat profile with an hourly time interval, based on; (a) *01.12 Bleekergeb. (Sorbonnelaan 4)*, (b) *01.23 Ornsteinlab. (Princetonplein 1)*, (c) *01.35 NITG-TNO (Princetonlaan 6)*, (d) *01.52 Buys Ballot lab. (Princetonpl. 5)*, (e) *01.58 Aardwetenschappen (Budapestlaan 4)*, *(f) 02.28 Res.kas+Bot.tuin (Uppsalaln Tuin)*, (i) *05.27 Univers.Bibliot (Heidelberglaan 3)*. 20

3.8 Expected thermal demand of UU with an hourly time interval of year 2018. The thermal profile is based on a various number of assumptions, which are discussed in Section 3.4.4 22

3.9 Schematic overview of the proposed scenarios and cases. (I) represents scenario one where UU only is an end user of electricity, where (II) represents the scenario where UU wants to decarbonise their whole energy supply. Scenario (I) is subdivided in two sub-scenarios (1) and (2). Sub-scenario (1) examines the energy system if no seasonal storage option is available and (2) when PtG is added in the set of technologies. Both sub-scenarios are investigated with (A) and without (B) wind turbine area constraint. Scenario (II) is also subdivided in sub-scenarios (3) and (4), at which (3) discusses the multi energy system if no geothermal heat is available and (4) if geothermal heat import is allowed. Identical as (1) and (2) are (3) and (4) also examined with (A) and without (B) wind turbine area constraint. For sub-scenario (4) two additional analyses are performed (C) where geothermal heat could be imported accompanied with zero emissions and (D) where geothermal heat could be imported at low cost accompanied with zero emissions. 25

4.1 Cost-emission Pareto front for sub-scenario 1 for electricity supply to UU with as available set of technologies; WTs, PV panels, and LiB for (1A) the campus property (1B) campus property with unlimited area for WTs. In this scenario only electricity import is allowed. 27
4.2 Size of the installed technologies along the Pareto fronts for scenario 1A (blue circle) and 1B (orange triangle): (a) PV panels, (b) 4500 kW WTs, (c) 2500 kW WTs, (d) 1500 kW WTs, (e) LiBs. Graph (f) shows the amount of imported electricity as a fraction of the total electricity demand. 29
4.3 Electrical output of the technologies that were included in the optimal design of scenario 1A for (a) in January and (c) in July for 30 % emission reduction and (b) in January and (d) in July for 80% emission reduction. 30
4.4 Electrical output of the technologies that were included in the optimal design of scenario 1B for (a) in January and (c) in July for 30 % emission reduction and (b) in January and (d) in July for 80 % emission reduction. 30
4.5 Amount of electricity stored over the year divided in scenario 1A and 1B, where Graph (a) represents the electricity stored for the 100% emission reduction and 80% emission reduction. The hourly electricity stored is based on the loess regression, which uses a local weighted regression to fit a smooth curve through the points, allowing to reveal trends and cycles of the electricity stored throughout the year. Graph (b) shows the battery storage for designs with 80% and (c) for 100% emission reduction. 31
4.6 Cost-emission Pareto front for sub-scenario 2 for electricity supply to UU with as available set of technologies; WTs, PV panels, LiB and PtG for (2A) the campus property (2B) campus property with unlimited area for WTs. In this scenario only electricity import is allowed. 32
4.7 Size of the installed technologies along the Pareto fronts for scenario 2A (blue circle) and 2B (orange triangle):(a) PV panels, (b) WT 4500, (c) WT 2500, (d) WT 1500, (e) PEMEC (f) Battery (g) H_2 PEMFC and (h) HOS. Figure (i) shows the amount of imported electricity as a fraction of the total demanded electricity. 34
4.8 Amount of electricity stored over the year divided in scenario 2A and 2B, where Graph (a) represents the electricity stored for 100% emission reduction and 90% emission reduction. The hourly electricity stored is based on the loess regression, which uses a local weighted regression to fit a smooth curve through the points, allowing to reveal trends and cycles of the electricity stored throughout the year. Graph (b) shows the electricity stored divided in the different energy carriers for designs with 90% and (c) for 100% emission reduction. 35

5.1 Cost-emission Pareto front for sub-scenario 3 for electricity and heat supply to UU with as available set of technologies; WTs, PV panels, LiB, PtG, edHP, boilers, industrial boilers, ST and HWTS for (3A) the campus property (3B) campus property with unlimited area for WTs. In this scenario only import of electricity and gas is allowed. 37
5.2 Size of the installed technologies along the Pareto fronts for scenario 3A (blue circle) and 3B (orange triangle):(a) PV panels, (b) WT 4500, (c) WT 2500, (d) WT 1500, (e) PEMEC and (f) H_2 PEMFC, (g) ST panels, (h) edHPs, (i) boilers and (j) industrial boilers. 40
5.3 Size of the installed technologies along the Pareto fronts for scenario 3A (blue circle) and 3B (orange triangle): (a) Battery, (c) HWTS and (e) HOS. Graph (b), (d), (f) represent the fraction imported electricity, heat and gas of the total energy demand. 41
5.4 Amount of energy stored over the year divided in scenario 3A and 3B, where Graph (a) represents the energy stored for 100% emission reduction and 90% emission reduction. The hourly energy stored is based on the loess regression, which uses a local weighted regression to fit a smooth curve through the points, allowing to reveal trends and cycles of the energy stored throughout the year. Graph (b) shows the energy stored divided in the different energy carriers for designs with 90% and (c) for 100% emission reduction. . 42
5.5 Cost-emission Pareto front for sub-scenario 4 for electricity and heat supply to UU with as available set of technologies; WTs, PV, LiB, PtG, edHP, boilers, industrial boilers, ST and HWTS for (4A) the campus property (4B) campus property with unlimited area for WTs. In this scenario import of electricity, geothermal heat and gas is allowed. 43

5.6 Size of the installed electricity and heat generating technologies along the Pareto fronts for scenario 4A (blue circle) and 4B (orange triangle) with (a) representing PV, (b) WT 4500, (c) WT 2500, (d) WT 1500, (e) PEMEC and (f) H2 PEMFC, (g) representing ST, (h) edHP, (i) boiler, (j) industrial boilers. 45
5.7 Size of the installed technologies storage technologies along the Pareto fronts for scenario 4A (blue circle) and 4B (orange triangle): (a) Battery, (c) HWTS and (e) HOS. Graph (b), (d), (f) represent the fraction imported electricity, heat and gas of the total energy used. 46
5.8 Cost-emission Pareto front for sub-scenario 4 for electricity and heat supply to UU with as available set of technologies; WTs, PV panels, LiB, PtG, edHP, boilers, industrial boilers, ST and HWTS for scenario (4C) the campus property and scenario (4D) also at campus property by import geothermal heat available at low costs. In this scenario import of electricity, geothermal heat and gas is allowed. Geothermal heat import is in this case accompanied with zero emissions. 48
5.9 Fraction of imported energy of total energy demand for scenario 4C and 4D, with (a) electricity, (b) geothermal heat and (c) gas. 49

6.1 Cost emission Pareto front for three scenarios assessing different areas available for PV and ST installation, namely: (i) Reference 1 289 014 m^2 (ii) 75 000 m^2 and (iii) 20 000 m^2 to determine the sensitivity of the systems costs for scenario 3A (Section 3.5). 51
6.2 Cost emission Pareto front for three scenarios assessing different prices for electricity import, namely: (i) Reference (ii) 25 % increase in price and (iii) 50 % increase in price to determine the sensitivity of the systems costs for scenario 3A (Section 3.5). 51
6.3 Cost emission Pareto front for three scenarios assessing different prices for electricity import, namely: (i) Reference (ii) 50 % increase in price and (iii) 100 % increase in price to determine the sensitivity of the systems costs for scenario 3A (Section 3.5). 52
6.4 Cost emission Pareto front for three scenarios assessing different thermal demand, namely: (i) Reference (ii) 43 % decrease in thermal demand and (iii) 43 % decrease in thermal demand to determine the sensitivity of the systems costs for scenario 3A (Section 3.5). 52

A.1 Map of USP, where the buildings in green, red and dark green are the buildings owned by UU. 63
A.2 Schematic presentation of the buildings connected to UU's own heat network. 66
A.3 Schematic presentation of the buildings connected to the existing ATES system in north west campus. . . 67

List of Tables

3.1 The area available for ST and PV panels of the current suitable solar roofs and solar parkings. Solar roofs are presented per m^2 per building and solar parkings per m^2 per parkinglot. 14
3.2 The frequency in which the electricity [E] and heat [Q] data is available is presented per building of UU. If hourly is stated in E data frequency or Q data frequency, indicates that data is available for 2018 with hourly time interval, zero means demand is zero, N/A data is unavailable, incomplete data is demonstrated with insufficient (in notes the parts missing are presented), profile indicates that a profile is used to determine the hourly demand. The column data used shows which of the data is used per building. Notes indicates the missing parts in case of insufficient data or whether an absorption chiller is present in the building. 16
3.3 The annual hand measured and the recorded heat consumption per building and the related factor that is used for Equation 3.6 to determine the annual actual hourly profile. The total factor is used to determine the annual actual profile with an hourly time interval for buildings where no hand measurements are done. 18
3.4 The total heat supply by the ATES system in kWh per connected building for the months January till March and the expected heat supply for December of year 2018. 21
3.5 The expected hourly heat supply by ATES system to connected buildings in kWh of the months January, February, March and December 2018. 21
3.6 List of the energy prices and emission factors for electricity, geothermal heat and gas. The emission factor of green energy is used during this research, which is based on 10% of the Dutch average emission factor of a particular energy carrier. The presented price and emission factors are allocated to imported energy in the E-Hub tool. 23

4.1 Relative cost increase per emission reduction achieved by the design compared to reference for scenario (1A) campus area and (1B) campus area with unlimited area for WTs. The bold value indicates the maximum emission reduction that can be achieved if electricity costs are not more than doubled. 28
4.2 Relative cost increase per emission reduction achieved by the design compared to reference for scenario (2A) campus area and (2B) campus area with unlimited area for WTs. The bold value indicates the maximum emission reduction that can be achieved if electricity costs are not more than doubled. 33

5.1 Relative cost increase per emission reduction achieved by the design compared to reference level for scenario (3A) campus area and (3B) campus area with unlimited area for WTs. The bold value indicates the maximum emission reduction that can be achieved if electricity costs are not more than doubled. . . . 38
5.2 Relative cost increase per emission reduction achieved by the design compared to reference for scenario (4A) campus area and (4B) campus area with unlimited area for WTs. The bold value indicates the maximum emission reduction that can be achieved if electricity costs are not more than doubled. 43
5.3 Relative cost increase per emission reduction achieved by the design compared to reference for scenario (4C) campus area with zero emission geothermal heat import and (4D) at campus area with zero emission geothermal heat import at low costs (6 EUR/GJ). The bold value indicates the maximum emission reduction that can be achieved if electricity costs are not more than doubled. 48

A.1 Expected annual electricity and heat demand of UU of year 2018 listed per building and the total annual energy supply by the existing PV panels and ATES system of UU. The total electricity demand of UU is determined by the sum of the demand of the buildings minus the PV generation. The total annual heat demand is the sum of the heat demand per building minus the ATES systems heat generation. The optimisations are performed based on this annual energy demand of UU. 64
A.2 The existing connections to UU heat network and ATES system listed per building. Yes indicates the building is connected, while no means there is no connection. 65

B.1 Input data for conversion and storage technologies in the E-Hub. In this case α represents the energy coefficient 1, β energy coefficient 2, γ energy coefficient 3, δ the size coefficient 1, ζ size coefficient 2, κ size coefficient 3, ν size coefficient 4 and ρ the first principle to electrical efficiency ratio. For storage technologies η represents the conversion or storage efficiency, Λ the time variation, Φ the storage loss coefficient, τ the storage charging/discharging time, Θ^{min} the minimum air temperature, Θ^{max} the maximum air temperature and p the pressure 69
B.2 Cost coefficients of conversion and storage technologies implemented in the E-Hub. In this case θ represents the cost coefficient 1, μ cost coefficient 2, S^{min} the minimum technology size, S^{max} the maximum technology size and ψ the fraction for maintenance costs 69

List of Abbreviations

General

COP	Coefficient of Performance
GO	Guarantees of Origin
MES	Multi Energy System
MILP	Mixed Integer Linear Programming
MIP	Mixed Integer Program
UU	Utrecht University
USP	Utrecht Science Park
RES	Renewable Energy Source
RET	Renewable Energy Technology

Technologies

ATES	Aquifer Thermal Energy Storage
edHP	electrical driven Heat Pump
HOS	Hydrogen Storage
HWTS	Hot Water Thermal Storage
LiB	Lithium Ion Battery
PV	Photo Voltaic panel
PtG	Power to Gas
PEMEC	Proton Exchange Membrane Electrolyser
PEMFC	Proton Exchange Membrane Fuel Cell
ST	Solar Thermal
WT	Wind Turbine

Chapter 1

Introduction

The European Commission promotes the use of renewable energy sources in order to meet their goal to obtain a decarbonised energy system by 2050 [1]. In terms of decarbonisation, the European Commission refers to a reduction of 80 - 95 percent in greenhouse gas emissions by 2050 compared to the levels of 1990 [1]. To meet this challenging target and to simultaneously ensure secure and affordable energy, adaptation is required in all energy sectors [2]. Companies and other organisations are urged to switch to a more sustainable way of their energy use. Currently, there are many initiatives to make The Netherlands more sustainable in its energy consumption. Many actors try to actively participate in the energy transition. The municipality of Utrecht is also progressive in its goals for the energy transition, as they aim to be carbon neutral by 2040 [3]. In the Energy Agenda of the Province of Utrecht, Utrecht Science Park (USP) is designated as an experimental area for sustainable energy which aims at developing a self-sufficient energy supply system. Utrecht University (UU), which is partly located at this science park, wants to accelerate their energy transition and therefore has the ambition to be carbon neutral by 2030 [4]. Alongside , they also have the purpose of supporting others their transition. For example, UU helps municipalities to develop smart roadmaps to help get rid of natural gas [5]. In addition, UU in combination with various parties is investigating the possibilities of building the first geothermal power plant in Utrecht [6]. To date, the heat provision of UU is provided by green gas import. Although UU is investigating in the possibilities to get rid of the gas, currently their own heat supply is for the vast majority gas-based. At the moment, the energy supply is provided by only a small share of renewable energy technologies (RES). For the remaining part, green gas and electricity is imported. To act as a role model in the energy transition, it is of interest that they get rid of the gas themselves and increase self-sufficiency by enlarge the share of local energy generation. However, the path that must be followed to have a energy system compliant with their ambitions is currently unknown.

The development of a Multi Energy System (MES) can be recognised as a promising option for future energy supply [7]. An MES allows different energy carriers to interact with each other in order to create better economic, technical and environmental performance compared to the current system in which it operates individually [2][8]. Furthermore, the emergence of non-dispatchable renewable energy sources like solar and wind requires storage to balance the fluctuations in energy production [9]. Optimisation of such a system can provide insights in correct proportions of storage system- and

power generation capacities. An integrated management system can coordinate these processes to satisfy demand. Various studies on this subject provide tools to analyse optimal designs for such an MES. However, many decision variables are involved in an optimisation of the design, resulting in long computation times. Simplification of functions in the system to limit the computation time often goes at the expense of the accuracy of the results. Currently, optimisation by using Mixed Integer Linear Programming (MILP) is often used. Many tools have been developed using MILP as the optimisation method for design and operation of an MES, due to its ability to reconstitute complicated systems in order to limit computation time [10]. In many of the currently available tools, the time horizon is based on design days, which is unsuitable for analysing seasonal storage. However, the implementation of seasonal storage systems in an MES with renewable energy sources is essential. For this purpose Gabrielli et al. (2018) [11] developed a modelling framework using MILP formulations based on the coupling of typical design days, which allows the integration of seasonal storage into the optimisation. With the current understanding and available optimisation tools, valuable insights can be obtained on how to design an MES for a specific area.

UU is currently fully committed to the combination of Aquifer Thermal Energy Storage (ATES) systems with heat pumps for heat supply in their new buildings [12]. According to real estate development plans, it is expected that heat demand will decrease by 60 percent by 2030 compared to 2016 [12]. This is due to reduced heat losses in better insulated buildings and through the ATES/heat pump combination for heat supply [12]. These developments will bring a shift from heat demand to electricity demand, resulting in a more electricity dependent energy system. The required electricity could be produced by renewable energy sources like wind or solar. It is therefore important to determine to what extent UU can implement these technologies on their own property.

1.1 Research questions

To achieve the objective stated above, the following research question is proposed:

What is the maximum emission reduction that can be achieved by generating energy locally at Utrecht University? And what is the most carbon-cost effective configuration?

In this case the boundaries of the design of the energy system proposed are limited to UU's own property. Carbon-cost effective design refers to the optimal design, at which a trade-off is made between costs and CO_2 emission reduction. Here, a limit value is chosen of a maximum of 2 times the reference price for energy. In order to answer the main question in this research, the below mentioned sub-questions are addressed:

I To what extend can Utrecht University decarbonise their electricity supply by generation and storage of **electricity** locally? And what is the most carbon-cost effective configuration?
This sub-question analyses the design of a carbon neutral system that only supplies electricity to UU, wherein the boundaries of the installed technologies are limited to the Campus's own site. The importance of renewable energy technologies (RET), such as photovoltaic panels and/or wind turbines for a carbon neutral electricity supply is examined with the required storage facilities.

It indicates whether it is possible, with the available land for energy generation, to supply up to 100% of total electricity demand using locally generated electricity.

II To what extend can Utrecht University decarbonise their **electricity** and **heat** supply by generation and storage of energy locally? And what is the most carbon-cost effective configuration? *UU aims to be self-sufficient and carbon neutral, in both their electricity and heat provision. Taking in mind the area limitations of the campus, this sub-question examines to what extent and in what manner this goal can be achieved.*

1.2 Relevance of the research

The results can provide a basis for the energy provision of UU to be further examined by their Energy Team. It indicates whether it is possible to install an autarkic energy system at UU campus, or whether it is more to their advantage to participate on larger scale renewable production projects, such as the geothermal project of Utrecht. A various number of decarbonisation options for UU are proposed, which can be implemented according their preference. Besides, the municipality of Utrecht can adjust their strategy to create a carbon neutral energy system for Utrecht based on the outcomes of this research, since the USP is seen as their test case. In addition, the quick wins become clear in terms of carbon-cost effectiveness. The presented methods and obtained optimisation results in this study can provide as a guide for other science parks, companies, cities and municipalities to create an MES.

1.3 Outline

The remainder of this thesis is structured as follows. In the second part, the theoretical framework is explained, which elaborates on MESs and discusses the key technologies within this research. The methodology section appoints the methodological approach in order to answer the main research question. The results are divided into two specific cases; (i) evaluation of the design of an energy system at which UU only obtains electricity from the system, and (ii) assessment of the design considering a local MES for their entire energy supply. Both scenarios are examined by use of two sub-scenarios. Subsequently, the results are discussed in the discussion section. Finally, the conclusion answers the research questions as stated above.

Chapter 2

Theoretical Background

2.1 Multi Energy Systems

The concept of Multi Energy Systems is important in this study, and is discussed in more detail. The following definition is considered for MES; a system whereby heat, cooling, electricity, fuels and other energy carriers optimally interact with each other in order to increase the economic, environmental and technical performance of the energy system [13] [14] [15] [8]. Multiple technologies in the MES convert multiple energy carriers, fossil fuels as well as renewable based sources, into demanded energy outputs like heating, cooling and electricity. The fact that different energy carriers can operate with each other, creates possible benefits for the overall system, for example energy efficiency can be improved as well as an increase in reliability and load flexibility. Alongside its optimisation potential, it also allows integration of renewable energy and creates possibility for synergies [16] [13] [2] [17]. Considered key technologies for the MES for UU are presented in the next section.

2.2 Key technologies

This section elaborates on the available conversion and storage technologies that are investigated for the MES for UU. An emphasis is placed on the characteristics of the technologies and the related effect it has on the entire system.

2.2.1 Conversion technologies

The considered conversion technologies are photovoltaic (PV) panels, solar thermal (ST) panels, wind turbines (WT), electrically driven heat pumps (edHP) and boilers. The listed technologies are selected based on UU's preference and/or its ability to generate electricity or heat without emitting CO_2 emissions.

Photovoltaic panels PV panels generate electricity from solar energy, by using PV cells. The PV cell is a semi conductor device that generates direct current electricity by use of solar irradiance [18]. PV panels are well-proven and widely installed over the whole world. A huge disadvantage is its dependency of the sun, resulting in day and season variability in the output of this technology.

Therefore, it should operate with a dispatchable electricity-producing technology or storage technology, here batteries and power to gas to be able to meet demand at any moment in time. The capacity of PV panels in the follow up chapters is presented in m^2. The amount of installed PV panels is limited by the area available for PV installation. The maximum electricity output of $1\,m^2$ of PV is approximately 1.2 kW.

Solar thermal Solar thermal panels generate heat by using the sun as energy source. In this case solar radiant energy is transferred to water, which flows through the collector [19] [18]. The solar radiant energy is in this way converted into usable heat. The integration of ST into district heating systems is being used more often over the years [20]. The hot water can be used by end consumers, for example for space heating. Identical to PV panels, its reliability depends on the weather conditions [21]. Therefore this technology also requires a dispatchable power or storage technology to supply heat to balance the mismatch between heat generation and use [22]. Possible examples are electrically driven heat pumps (edHP) and/or boilers as dispatchable technology and Hot Water Thermal Storage (HWTS) as storage. The capacity of ST is presented in m^2. The maximum units installed depends on the area available for solar technologies, making this technology competitive with PV.

Wind turbines In this case electricity is generated by using the wind as energy source. Kinetic energy arrives the blades and is subsequently converted into mechanic energy. By the use of a generator the mechanic energy is converted into electrical energy [18]. Wind speeds have to exceed the cut-in to generate power, since from this point the rotor starts to function. Between the cut-in and the rated wind speed, the generated power enlarges. From the rated till the cut-off wind speed the generated power remains equal. The wind turbine is shut off when wind speed exceeds the cut-off speed. The operation of the WT is at its highest underneath a constant wind speed between the rated and cut-off wind speed [23]. Similar to the above mentioned technologies, wind is also a non-dispatchable energy source. To ensure reliable electricity supply a storage technology or dispatchable energy is required. However, the storage options needed tend to be more day to day storage rather than seasonal. The capacities considered in this research are 1500 kW, 2500 kW and as largest 4500 kW. The constraint on the number of possible turbine installation is calculated with a radius of 420 m around each tower. This value is determined based on a various number of studies and validated based on existing wind turbine projects. On average, the area a wind turbine occupies is six times the blade length. In this case, it is assumed that the blade length of the three proposed wind turbines are equal. Furthermore it is expected, that wind turbines and solar based technologies are not competitive in the available area.

Electrically driven heat pump An electrically driven heat pump (edHP) generates heat by use of electricity and are widely used for space heating [24]. Heat pumps draw heat from the ambient and convert it to higher temperatures [22]. The performance is thus influenced by the air temperature, which affects efficiency. If this technology runs on carbon free electricity, the heat supplied is emission free.

Boiler A boiler generates heat by burning natural gas to heat up water. Despite the unsustainable nature of this technology, this technology is included in the analysis, since this technology is used for the current heat production in combination with green gas.

2.2.2 Storage Systems

Both heat and electricity storage technologies are considered. Storage options with an electrical input are the battery (LiB) and Power to Gas (PtG), while Hot Water Thermal Storage (HWTS) and Aquifer Thermal Energy Storage (ATES) operate with a thermal input power.

Batteries The term battery refers to a Lithium ion Battery (LiB). LiBs are commonly used because the storage option is characterised by high power density, high energy density and long life [25][26]. LiBs are mainly used for short term, day-to-day storage. This is mainly due to its self discharge which makes it unsuitable for seasonal storage [27]. However, LiBs have good potential to provide or store electricity in case of a mismatch between demand and RET production.

Power to Gas Power to Gas refers to a three stage process whereby hydrogen is (i) produced by use of electricity, (ii) stored and (iii) converted back into electricity and/or heat. The first process is performed by a proton exchange membrane electrolyser (PEMEC). The PEMEC uses electricity to dissociate water into hydrogen and oxygen, which can subsequently be stored in hydrogen tank storage (HOS) [28]. This operation can be performed at times of an electricity surplus. The hydrogen stored can, at times of an energy shortage, be converted back to electricity or heat by use of the proton exchange membrane fuel cell (PEMFC). Negligible energy losses in the hydrogen tanks ensure that this technology can be used for seasonal storage.

Hot Water Thermal Storage While there are two forms of HWTS, latent and sensible, this paragraph only considers the sensible HWTS. This is due to its lower costs and higher technological maturity. In this case hot water is stored in storage tanks at 90 ∘C and cooled to 65 ∘C [11]. HWTS is commonly used for short term thermal heat storage, due to its respectively high energy losses and low energy density [29].

Aquifer Thermal Energy Storage This technology is used as seasonally storage. Thermal energy can be stored for either cooling or heating purposes [30]. Ground water is pumped back and forth to cool or heat buildings [31]. Heat is subtracted in summers by using direct heat exchange in the vertical wells and infiltrated in the system for usage in winters and visa versa [22][32]. Due to the low working temperature of this technology, ATES is often used in combination with a heat pump to increase thermal output [22]. Despite its low output, this technology has been frequently used for space heating for over the past 20 years [32] [30].

Chapter 3

Methodology

3.1 The E-Hub

The Energy-Hub is used to conduct this research, an existing tool that allows to determine the optimal design of an MES for a specific area. MATLAB is used as programming software with Gurobi Optimization as solver [33]. The tool was built upon the Energy Hub concept of Geidl (2007) [13] which formulates the in- and output power flows of a hub by a set of matrix formulations [16]. The formulations used are composed by using Mixed Integer Linear Programming (MILP), Section 3.3 elaborates on the principles of this method. The linear models used are based on the modelling framework compiled by Gabrielli et al. (2018) [11] and Gabrielli et al (2018a)[10]. Typical design days are applied in this framework, which drastically reduced the computation time. In this case, the operation variables are separated into two groups, those which are related and unrelated to binary variables. The related are defined for every hour of the year, while the unrelated are reduced in number by implementing typical design days. Typical design days are applied in this research, where 48 typical design days is seen as a reasonable trade-off between the reliability of the results and the related computation time [11]. In case a distributed energy system is analysed, multiple hubs (e.g. nodes) could interact through a network of different energy carriers. This function of the tool is not used during this study, since the optimisations are performed with one node. This simplification is made since the electricity network, and also a large part of the heat network is already in place. Besides, the approach of this work is primarily based on indicating the maximum achievable in terms of local generated carbon free electricity. Determination of the design is therefore essential, instead of the load distribution through a network to the connected buildings. The optimisations in this research are computed with an MILP-gap of 0.01 and 48 typical days using the multi objective optimisation approach (Section 3.3.2), unless otherwise is stated. The proposed matrix-based model reports on technology selection, size, operation and costs. The current version of Energy-Hub is preferred during this study considering its comprehensive set of renewable technologies, with reference to WTs, PV panels, ST panels, edHPs, HWTS, PtG, boilers and LiB. The information relevant to UU is reconstructed and implemented in the E-Hub, whereby the results made it possible to make a prediction about the optimal configurations of the design of a decarbonised energy system.

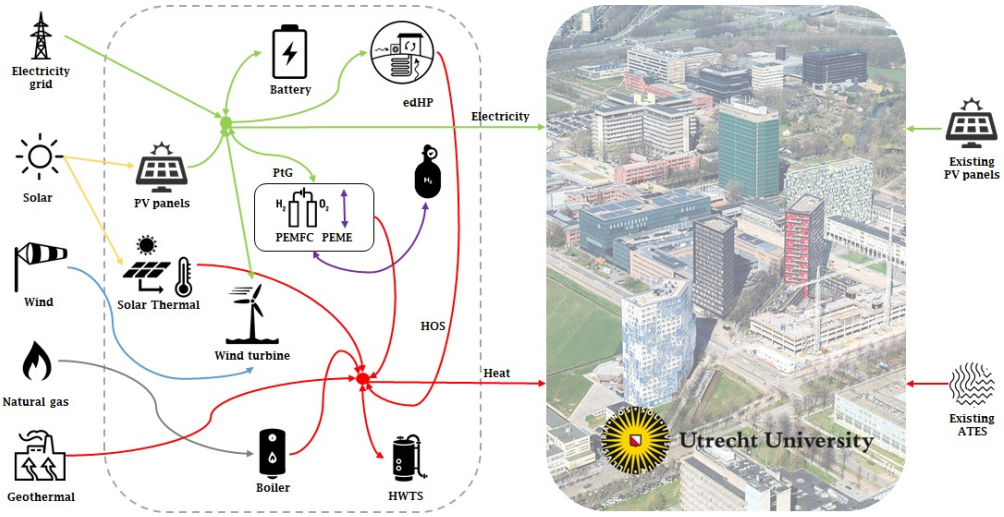

Figure 3.1: Schematic representation of the investigated system supplying heat and electricity to the end user Utrecht University. Green lines represent electricity transfer, yellow solar irradiance, blue wind energy, red heat, grey natural gas and purple hydrogen. The available set of technologies in the E-Hub relevant to analysis for UU are PV panels, ST, WTs, HWTS, PtG, HOS, LiBs, edHPs. Existing PV panels and ATES systems are excluded as technologies in the optimised systems, since the operation of the two technologies are processed in the demand.

3.2 System Description and optimisation problem

The considered MES aims to deliver the hourly demanded energy to the end user, in this particular case, UU located at Utrecht Science Park (USP) at the eastern of Utrecht. The USP is owned by UU, however multiple companies and schools are established on this campus as well. Although they are located at USP, third parties are not participating as end users in the considered designs. Appendix A.1 represents a map of Utrecht Science Park, which shows the buildings owned by UU. The considered MES could be connected to different types of grids, such as electrical, heat and gas grid. Mainly renewable based conversion technologies and storage units are examined for the energy system. The analysed configurations are discussed in Section 3.5. Figure 3.1 provides an schematic overview of the available technologies of the Energy Hub which were examined for the considered energy system. The existing ATES system and PV panels are excluded in the optimisation of the design since the energy supply by these technologies is incorporated in the demand.

3.2.1 Objective function

The objective of the optimisation problem to be minimised is total annual costs J, consisting of the sum of the capital costs J_c (Equation 3.1), operational costs J_o (Equation 3.2) and maintenance costs J_m (Equation 3.3) of the total system. In addition to the cost objective, the optimisation problem can also be optimised in terms of CO_2 emissions, this by minimising Equation 3.4, which is explained later on.

$$J_c = \sum_{i \in \mathcal{M}} (\lambda_i \cdot S_i + \mu_i)\omega_i \tag{3.1}$$

In Equation 3.1 the variable and fixed costs coefficient are respectively λ and μ for the i-th technology, with $\mathcal{M}$ being the set of all technologies. The unit size for the i-th technology is indicated with S_i, where ω represents the annuity factor. In this case the annuity factor is calculated with an interest rate of 6 %.

$$J_o = \sum_{j \in \mathcal{N}} \sum_{t=1}^{T} (u_{j,t} \cdot U_{j,t} - v_{j,t} \cdot V_{j,t}) \tag{3.2}$$

Operational costs are related to the amount of imported and/or exported energy. In this case u and v are the import and export prices and U and V are the amount of imported and exported energy of a specific energy carrier j and point in time t. $\mathcal{N}$ is the set of all nodes, and T is the time horizon.

$$J_m = \sum_{i=1}^{M} \psi_i \cdot J_{c,i} \tag{3.3}$$

The annual maintenance costs are formulated based on a fraction of the annual capital costs. The fraction is defined by ψ_i, which is technology specific and includes all other factors like labor costs, materials etc.

In addition to the main objective, the model can be assessed based on the environmental performance. Therefore, the optimisation problem is constrained by an upper limit of by CO_2 emissions. The annual emissions is formulated in Equation 3.4. :

$$e = \sum_{j \in \mathcal{N}} \varepsilon_j (\sum_{i \in \mathcal{M}} \sum_{t=1}^{T} U_{j,i,t}) \tag{3.4}$$

The ε represents the CO_2 rate of a specific energy carrier j. Section 3.4.4 *Energy prices and emission factors* elaborates on the emission factors used in this study.

Input variables Inputs for the optimisation problem are (i) prices and CO_2 rates for different imported/exported carriers, (ii) weather conditions containing temperature, solar irradiance and wind speed and (iii) the expected energy demand, all with an hourly resolution on a one year time horizon. Section 3.4 elaborates on the input data used during this study.

Decision variables The output is the optimal design and operation of the system. The following decision variables are returned from the model (i) the capacity/size of the installed technologies (ii) the operational schedules and on/off-status of the technologies, (iii) the amount of stored energy in storage technologies and (iv) the amount of imported or exported energy from or to the grid.

Constraints The following constraints are applied to the optimisation model (i) carrier constraint, which are related to the amount of imported/exported energy and CO_2 emissions, (ii) furthermore component constraints which applies to the performance of conversion and storage technologies, (iii) area constraints which limits the amount of installed squared meters of PV and ST and units of WTs, (iv) network constraints expresses the maximum flows of the network and (v) the energy balance which ensures that the sum of all generated and/or imported energy is equal to the sum of all used

and/or exported energy. With regard to the mathematical formulations used for the component and network constraints, reference is made to the papers of Gabrielli et al (2018) [11] and Gabrielli et al (2018a) [10]. The related technological specific values used in the current E-hub model are presented in Appendix B.1 and B.2, representing coefficients used related to cost and operation.

3.3 Mixed Integer Linear Programming

For designing an energy system it was important to determine the capacities, on/off status, operation schedules and load allocation corresponding to the demand of the end user. The Mixed Integer Linear Programming approach allows to calculate above mentioned. Recently the MILP approach is a recognised method for energy system optimisation and is widely utilised [34]. This approach is most preferred in energy system optimisation due to its ability to determine units with discrete numbers and due to linearisations of functions which considerably reduces the computational time.

The MILP (Equation 3.5) is formulated in MATLAB 2018b using YALMIP [35] and solved with Gurobi v8.02 [33] by branch and bound algorithm on an Intel Xeon E5-1620 3.60 GHz machine with 16 GB RAM.

$$\begin{aligned} \min_{x} \quad & \mathbf{c}^T \mathrm{x}, \mathrm{y} + \mathbf{d}^T \mathrm{y} \\ \text{s.t.} \quad & \mathbf{A}\mathbf{x} + \mathbf{B}\mathbf{y} = \mathbf{b} \\ & \mathbf{x} \geq 0 \in \mathbb{R}^{\mathbf{N_x}}, \mathbf{y} \in \mathbb{N}^{\mathbf{N_y}} \end{aligned} \tag{3.5}$$

In the formulation, the abbreviations $\mathbf{c}$ and $\mathbf{d}$ represents the cost vectors related to $\mathbf{x}$ and $\mathbf{y}$, which are continuous and binary decision variables. A and B are the related constraint matrices and b is the constraint known-term. $\mathbf{N_x}$ indicates the dimension of $\mathbf{x}$ and $\mathbf{N_y}$ for $\mathbf{y}$, respectively. A detailed explanation can be found in Gabrielli et al. (2018a) [10].

3.3.1 Branch and Bound

Branch and bound method uses intelligent enumeration to solve the MILP problem, by constructing a number of sub-problems [36]. First, the integrality constraints of the initial MIP are relaxed, by the so-called root relaxation, where the binary values are assumed to be continuous values, creating a linear optimisation. The algorithm produces an optimal solution for the relaxation, where some of the integer-constrained variables assuming fractional values [36]. Such a variable, also called *branching* variable is chosen and *branched on*. In this case two sub MIPs are created where the branching variable is constrained by a *upper branch* and *lower branch*, which are integer values. For example, *branching* variable x is set as $x_i \geq 4$ and ≤ 5, formulating two MIPs. The same procedure as described above is applied to the two new MIPs. Applying this approach multiple times a the so-call *search tree* is created, where the MIPs are seen as *nodes*. The solver Gurobi disposes, in case of unfeasibility, or solves the MIPs if the solution complies with the initial MIP integrality constraints. In short, the solver constructs a sequence of sub-problems that merge to a solution of the MIP. When a feasible solution is found, the node is assigned as *fathomed*. Branching this node is no longer necessary. If the fathomed node has the best solution found. The information provided by this node is analysed,

at which the best integer solution found at any point is selected as the *incumbent*. Heuristics are implemented in Gurobi to find the best incumbent as quickly as possible. The objective value of the incumbent is seen as the upper bound in case of a minimisation problem. The *best bound*, or in case of minimisation *lower bound* is obtained by taking the minimum of the optimal objective values of all current leaf nodes. The difference between the lower and the upper bound is indicated by the *gap*. A gap of zero means that the optimal outcome is reached. However, a gap limit for optimality is defined [33]. In the energy system optimisations in this research a gap limited of 0.01 is used.

3.3.2 Multi objective approach

The optimisation of the proposed energy system for UU is performed with a multi objective approach, which is solved by the ϵ constraint method [37]. In this way, a trade-off can be made based on costs and emissions. Two single-objectives are performed, one minimising total costs and one minimising total emissions, whereby emissions related to the total cost objective represent the maximum value of emissions. Based on these limits, the emission interval is divided into ten identical steps. Per step, a single objective minimising total annual costs is solved, where an emission threshold is implemented as a constraint. During this study, each point in the Pareto front corresponds with an optimal design. The optimal designs are plotted against emission reductions percentages and costs. The emission reduction that can be achieved by implementing a certain design is determined by dividing the emission of the optimised system by the emissions of the reference. In this case the reference emissions imply the emissions related to operation of the current system of UU.

3.4 Input data

This section describes the input data used for the optimisation, with a subdivision made in weather data, spatial limitations, current installations, demand data, energy prices and emission factors corresponding to UU.

3.4.1 Weather data

Weather station De Bilt is the nearest station to UU, therefore data of this weather station is used to ascertain the expected operation of WTs, edHPs, ST and PV panels. An hourly profile of the temperature, wind speed and solar irradiance of 2018 is presented in Figure 3.2 [38].

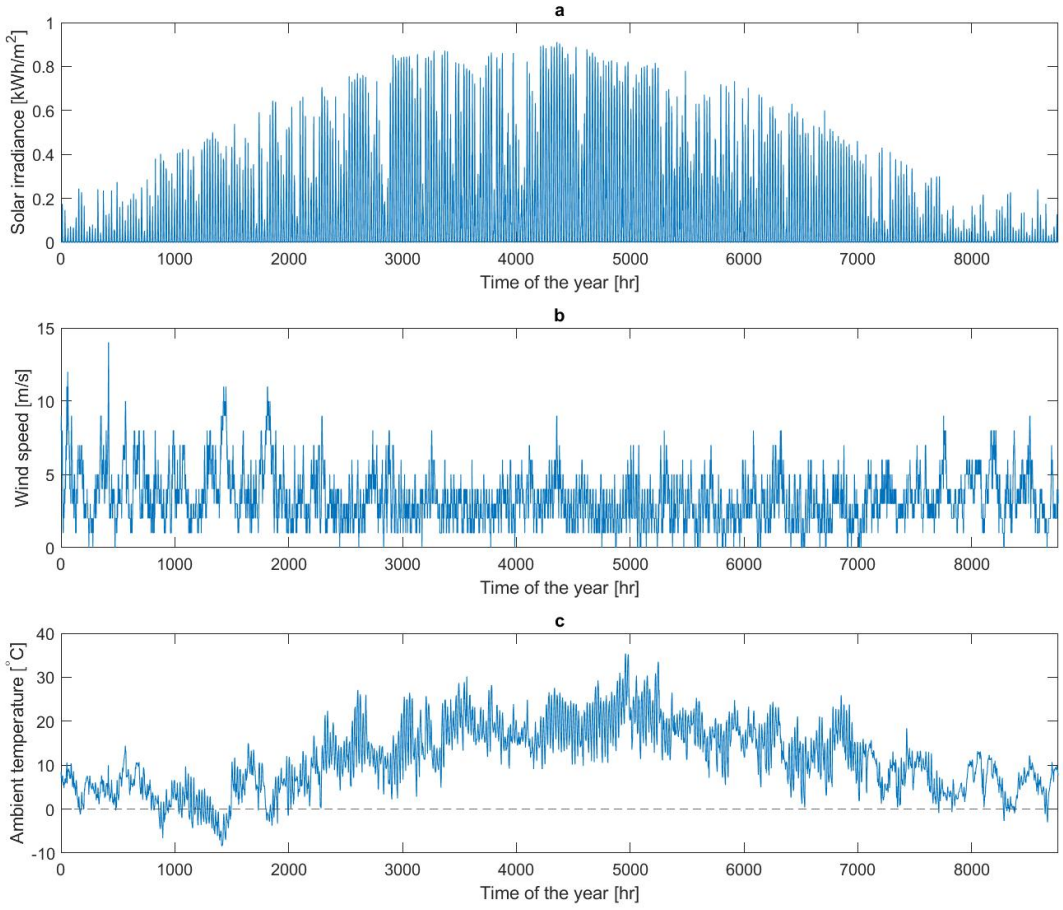

Figure 3.2: Weather data of weather station De Bilt with an hourly frequency of 2018, with (a) the solar irradiance in $\mathrm{kW\,h\,m^{-2}}$, (b) the wind speed in $\mathrm{m\,s^{-1}}$ and (c) the ambient temperature in °C.

3.4.2 Current installations

UU possesses two boiler houses, *Ketelhuis Princetonlaan* and *Ketelhuis Diergeneeskunde*. Considering UU consumes green gas, these installations can also be used for supplying carbon neutral heat. The capacity of *Ketelhuis Princetonlaan* is 30 MW, consisting of 3 installed units of each 10 MW, supplying heat at 110°C. The *Ketelhuis Diergeneeskunde* has a capacity of 18 MW, consisting of 3 boilers of 6 MW each supplying heat at 160°C. The boilers are connected by a heat network to UU buildings. Table A.2 in Appendix A.3 shows which of the buildings are connected to this network, based on Figure A.2 which outlines UU heat network at the campus. Besides the boilers, UU owns two ATES systems, one located in north west and one in south east. The ATES north west is linked to some of the buildings located at the west campus. The ATES south east is only used for third parties at this point, given that the existing buildings of the university in that area are not suitable in terms of isolation to connect to this system. Therefore, the south east system is not included for the analysis. Appendix A.3.2 shows the connected buildings to the nort west ATES system. However, the ATES system is not modelled in the tool, the operation of this storage technology is assimilated in the heat demand; on which Section 3.4.4 elaborates on the methodological steps taken to compute the ATES operation. In 2016, 4600 PV panels are installed with an 1.2 MW_p output [39]. According to the measuring systems of UU Energy Team the generated output of the PV panels of 2018 is approximately 1.075 $GW\,h\,yr^{-1}$. Furthermore, UU is equipped with 8 heat pumps, having a total capacity of 2469 kW_{th}. The technologies are mainly located in the buildings in north west campus. In this study, the existing industrial boilers and edHPs are implemented in the E-Hub tool, by assigning zero costs for installation of the existing capacities.

3.4.3 Spatial limitations renewables

The generation of renewable energy from areas outside USP is undesirable for UU's energy transition. Therefore, area boundaries for solar technologies and wind turbines are covered in this section. The data used is based on three advisory reports obtained by the Energy Team of Utrecht University, *Een zonnige toekomst, Plaatsmaken voor PV* and *Duurzame energie uit wind op de Uithof* [40][41][42]. Below the information relevant to the area constraints of the campus is listed, per renewable technology.

Use of solar technologies

Data concerning the solar energy constraints in this area is based on *Een zonnige toekomst* [41] and *Plaatsmaken voor PV* [40]. The aim of these policy visions is to guide the choices made by UU with regard to the implementation of PV in the period between 2018-2030. The follow up sections describes the available locations for PV and ST panels, whereby a distinction is made in solar roofs, solar parkings and solar fields. The areas have been determined by use of an area calculator [43].

Solar roofs and parkings Current suitable roofs: TNO building, R & O Building, Schimmelbuilding, Part of David de Wiedbuilding, Tolakker cattle shed. Possibly suitable in future: Ornsteinlaboratorium, Marinus Ruppertbuilding, Administration Building, other Tolakker cattle sheds, Victor J. Koningsbergerbuilding, Olympos, Schimmelbuilding, Groenmanbuilding, Jakobbuilding. Parking

lots that are covered with solar panels are called solar parkings. Long-term suitable parking lots are: Sorbonnelaan, Padualaan, Bolognelaan, Jenalaan and Willem C. Schimmelbuilding. The surface of the total amount of roofs available for solar panels is $0.09\,\mathrm{km}^2$. Table 3.1 shows the available square meters for PV.

Solar fields The currently suitable areas for solar fields, parkings and roofs are shown in green, blue and yellow (Figure 3.3). The suitable solar fields have surface of approximately $1.19\,\mathrm{km}^2$. The total available area for ST and PV of $1.29\,\mathrm{km}^2$ is the sum of the solar roofs, parkings and fields.

Table 3.1: The area available for ST and PV panels of the current suitable solar roofs and solar parkings. Solar roofs are presented per m^2 per building and solar parkings per m^2 per parkinglot.

Roofs	Surface	Parking lots	Surface
01.23 Ornsteinlab. (Princetonplein 1)	$2134\,\mathrm{m}^2$	Sorbonnelaan	$13\,170\,\mathrm{m}^2$
01.35 NITG-TNO (Princetonlaan 6)	$6220\,\mathrm{m}^2$	Jenalaan	$5950\,\mathrm{m}^2$
01.72 OWC: V.Koningsberger (Budap.ln2)	$1670\,\mathrm{m}^2$	Padualaan	$7830\,\mathrm{m}^2$
02.60 D.de Wiedgeb (Universiteitswg 99)	$2800\,\mathrm{m}^2$	Willem C. Schimmel	$4747\,\mathrm{m}^2$
03.85 S Groenmangeb CGN (Padualn 14)	$1805\,\mathrm{m}^2$	Bolognelaan	$755\,\mathrm{m}^2$
04.48 M.Ruppertgeb./Tr.1(Leuvenlaan 21)	$5365\,\mathrm{m}^2$		
04.42 Bestuursgebouw (Heidelberglaan 8)	$4950\,\mathrm{m}^2$		
07.07 Klin. Gez.dieren/Jakob (Yaleln 8)	$9085\,\mathrm{m}^2$		
07.22 R&O gebouw (Jenalaan)	$270\,\mathrm{m}^2$		
07.35 Klin. Heelk./Schimmel (Yaleln 112)	$13\,853\,\mathrm{m}^2$		
07.50 Jongveestal(Tolakker)	$6474\,\mathrm{m}^2$		
92.64 Olympos (Uppsalalaan 3)	$7415\,\mathrm{m}^2$		
Total	$62\,001\,\mathrm{m}^2$	Total	$32\,452\,\mathrm{m}^2$

Figure 3.3: Aerial view of Utrecht Science Park with the locations of the currently suitable solar fields, parking lots and solar roofs. The fields are marked in green, parkings in blue and roofs in yellow. The red area represents the unsuitable area solar fields.

Use of wind turbines

To determine the spatial limitations for the application of WTs the same area is used as the area available for solar fields Figure (3.3). According to *Duurzame energie uit wind op de Uithof*, the area available for wind turbines largely corresponds to the solar fields [42]. Therefore, it is assumed that the available area for solar fields is equal to the available area for WTs. Besides, PV or ST and WTs are not competitive since both technologies could be installed in the same area.

3.4.4 Demand

For the campus, it was only possible to obtain the energy demand of electricity and heat of 2018. Cooling demand is therefore excluded in the analysis. The data is obtained by the use of two databases, Eview [44] and Erbis [45], for which access is granted by the Energy Task force of Utrecht University Real Estate and Campus. Table 3.2 provides an overview of the data used. The follow up sections elaborate on its content. The annual electricity and heat demand that is applied in the optimisation is presented in Table A.1 of Appendix A.

Table 3.2: The frequency in which the electricity [E] and heat [Q] data is available is presented per building of UU. If hourly is stated in E data frequency or Q data frequency, indicates that data is available for 2018 with hourly time interval, zero means demand is zero, N/A data is unavailable, incomplete data is demonstrated with insufficient (in notes the parts missing are presented), profile indicates that a profile is used to determine the hourly demand. The column data used shows which of the data is used per building. Notes indicates the missing parts in case of insufficient data or whether an absorption chiller is present in the building.

Building	E data frequency	Q data frequency	Data used	Notes
01.12 Bleekergeb. (Sorbonnelaan 4)	Hourly	Hourly	Q & E	-
01.23 Ornsteinlab. (Princetonplein 1)	Hourly	Hourly	Q & E	-
01.26 ESL/v.d. Graaff. (Princetonlaan 4)	Hourly	zero	E	-
01.32 Minnaertgebouw (Leuvenlaan 4)	Hourly	insufficient	E	Q from 7700 h
01.35 NITG-TNO (Princetonlaan 6)	Hourly	Hourly	Q & E	-
01.52 Buys Ballot lab. (Princetonpl. 5)	Hourly	Hourly	Q & E	-
01.58 Aardwetenschappen (Budapestlaan 4)	Hourly	Hourly	Q & E	-
01.67 V. Meinesz B (Princetonlaan 8)	Hourly	insufficient	E	Q till 2000 h
01.72 OWC: V.Koningsberger (Budap.ln2)	Hourly	Profile	Q & E	-
01.74 ACCU (Budapestlaan 8)	Hourly	Profile	Q & E	-
01.77 Vening Meineszgebouw A (GEO)	Hourly	N/A	E	-
01.83 Wiskunde gebouw (Budapestlaan 6)	Hourly	zero	E	-
02.14 Fort Hoofddijk (Budapestlaan 17)	Hourly	Hourly	Q & E	-
02.28 Res.kas+Bot.tuin (Uppsalaln Tuin)	Hourly	Hourly	Q & E	-
02.60 D.de Wiedgeb (Universiteitswg 99)	Hourly	Hourly	Q & E	absorption chiller
03.77 Hugo Kruytgebouw (Padualaan 8)	Hourly	Hourly	Q & E	absorption chiller
03.85 S Groenmangeb CGN (Padualn 14)	Hourly	Profile	Q & E	-
03.89 Bloembergen geb.(Padualaan 12)	Hourly	zero	E	-
04.05 Educatorium (Leuvenlaan 19)	Hourly	Profile	Q & E	-
04.12 vUnnikgeb /Tr 2 (Heidelbergln 2)	Hourly	Profile	Q & E	-
04.42 Bestuursgebouw (Heidelberglaan 8)	Hourly	Profile	Q & E	-
04.48 M.Ruppertgeb./Tr.1(Leuvenlaan 21)	Hourly	Profile	Q & E	-
05.16 Langeveld geb (Heidelberglaan 1)	Hourly	N/A	& E	-
05.27 Univers.Bibliot (Heidelberglaan 3)	Hourly	Hourly	Q & E	-
07.07 Klin. Gez.dieren/Jakob (Yaleln 8)	Hourly	Hourly	Q & E	-
07.15 JDonker-Voet geb(Yaleln 104-106)	Hourly	N/A	E	-
07.24 Landb.dieren/de Bruin (Yaleln.7)	Hourly	insufficient	E	Q from 2200 h
07.35 Klin. Heelk./Schimmel (Yaleln 112)	Hourly	Hourly	Q & E	-
07.50 Jongveestal(Tolakker)	Hourly	N/A	E	-
13.22 Androclusgebouw (Yaleln 1)	Hourly	Hourly	Q & E	absorption chiller
13.25 Nw Gildestein (Yaleln 2)	Hourly	insufficient	E	-
13.54 Alexander Numan geb.(Yaleln.40-60)	Hourly	Hourly	Q & E	-
13.64 LSI (Yalelaan 62)	N/A	Profile	Q	-
92.64 Olympos (Uppsalalaan 3)	Hourly	Profile	Q & E	-

Electricity

As can be seen in Table 3.2 there is a lack in the electricity demand of Building *13.64 LSI (Yalelaan 62)*. The electricity use of this building is excluded for the analysis. The PV production of the current installed panels is presented in Figure 3.4. The PV production is deducted from the electricity consumption to determine the current electricity demand. The applied electricity profile of UU is presented in Figure 3.5. As expected, there is a clear difference in day and night usage and weekend and working days. The two outliers are probably caused by a power failure or a failure in the measurement systems.

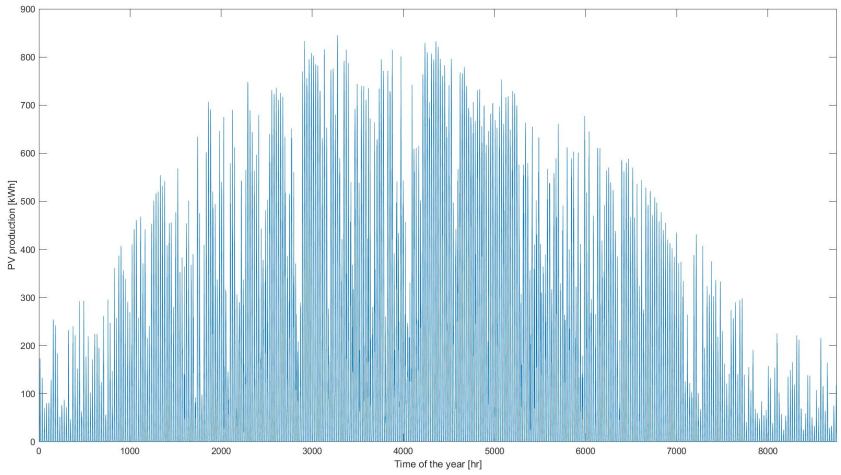

Figure 3.4: The PV production by the existing PV panels is presented with an hourly time interval of 2018. The electricity is produced by 4600 PV panels which are located at roofs of UU buildings. The peak performance of the installed PV panels is 1.2 MW_p.

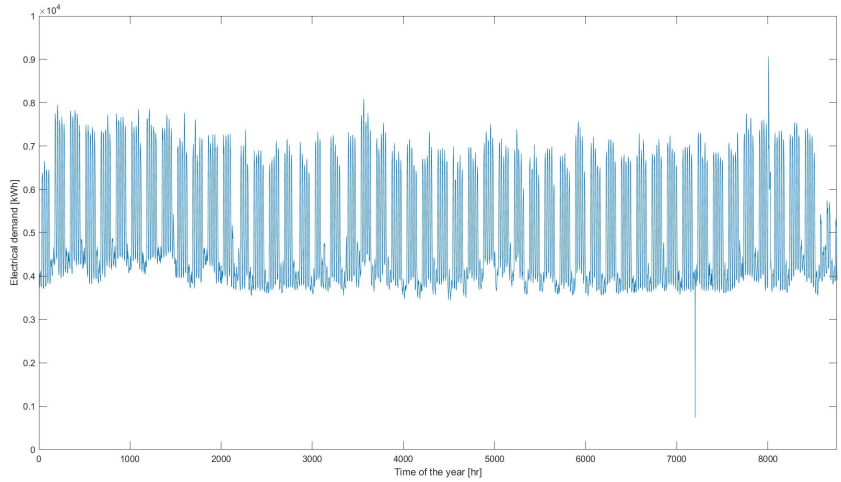

Figure 3.5: The expected electrical demand of UU with an hourly time interval of 2018. The electricity profile is the sum of the demand of UU buildings minus the generated electricity of the existing PV panels installed at UU.

Heat

Due to outdated heat measuring systems, it is necessary to make a number of assumptions. Four circumstances have occurred at processing the heat input data of UU; (i) there were differences between recorded data and hand measurements, (ii) not all data was registered with an hourly frequency, (iii) data was partly missing or even no data was available (iv) a number of buildings made use of an ATES system for which no operational profiles with an hourly frequency were accessible. The following paragraphs elaborate on the steps that were taken to ensure reliable data for the analysis.

Hand measures versus recorded data UUs heat measuring system is based on a pulse system. However this way of measurement is unreliable, since sometimes pulses are not registered. This resulted in differences in the recorded heat consumption and the actual heat consumption. Recorded values are available with an hourly frequency, while hand measurements are done once per month. Therefore, recorded values need to be multiplied by a factor to determine the actual heat consumption with an hourly time interval. This factor is calculated by the dividing the annual actual heat consumption by the annual recorded heat consumption. In this case only data of buildings is used where both hand measures and recorded data are available. In Table 3.3 the buildings used, in order to determine this factor, are presented.

The equation for the factor coefficient that is used to determine the actual heat consumption per hour per building is presented below in Equation 3.6.

$$Factor_{Building\ X} = Q_{Actual\ Annual,\ Building\ X} / Q_{Recorded\ Annual,\ Building\ X} \tag{3.6}$$

By multiplying the recorded hourly data for heat consumption by this factor, the actual hourly heat consumption is determined. The total factor coefficient is used for buildings where no hand measures are done but hourly recorded data is available. This applies to the following buildings: 07.07 Klin. Gez.dieren/Jakob (Yaleln 8), 07.35 Klin. Heelk./Schimmel (Yaleln 112) and 13.54 Alexander Numan geb.(Yaleln.40-60).

Limited availability of hourly data - For certain buildings only monthly data is available. To determine the hourly demand, a generic profile has been set up. In Figure 3.6 the profiles of 10 buildings are shown. For these buildings both hourly data is recorded and monthly hand measures are done.

As seen, there is a clear difference in summer and winter, as well as in day and night. However, the profiles Graph (g) and (j) of Figure 3.6 show the opposite, this is due to the presence of an absorption

Table 3.3: The annual hand measured and the recorded heat consumption per building and the related factor that is used for Equation 3.6 to determine the annual actual hourly profile. The total factor is used to determine the annual actual profile with an hourly time interval for buildings where no hand measurements are done.

Building	Annual actual	Annual recorded	Factor
01.12 Bleekergeb. (Sorbonnelaan 4)	504 722 kW h	393 056 kW h	1.2841
01.23 Ornsteinlab. (Princetonplein 1)	1 431 111 kW h	1 243 611 kW h	1.1508
01.35 NITG-TNO (Princetonlaan 6)	1 501 111 kW h	147 667 kW h	1.0166
01.52 Buys Ballot lab. (Princetonpl. 5)	2 705 278 kW h	2 526 389 kW h	1.0708
01.58 Aardwetenschappen (Budapestlaan 4)	966 389 kW h	1 084 722 kW h	0.8909
02.28 Res.kas+Bot.tuin (Uppsalaln Tuin)	2 190 278 kW h	1 775 833 kW h	1.2334
02.60 D.de Wiedgeb (Universiteitswg 99)	4 171 944 kW h	4 065 556 kW h	1.0262
03.77 Hugo Kruytgebouw (Padualaan 8)	9 121 111 kW h	9 152 222 kW h	0.9966
05.27 Univers.Bibliot (Heidelberglaan 3)	2 148 056 kW h	2 189 167 kW h	0.9812
13.22 Androclusgebouw (Yaleln 1)	10 030 000 kW h	9 813 333 kW h	1.0221
Total	34 770 000 kW h	33 720 556 kW h	1.0311

cooling installation. Less visible in this graph is the absence of an absorption chiller in the Hugo R. Kruyt building (Figure 3.6(h)). Due to the inefficiency of these installations, the profiles of (g)(h)(j) of Figure 3.6 are excluded for the determination of the generic heat profile.

In Figure 3.7, the generic heat profile is presented. This profile is determined by adding up the profiles of building Graph (a), (b), (c), (d), (e), (f) and (i) of Figure 3.6 divided by the sum of the annual heat consumption of the buildings (Equation 3.7). In this case time frequency t is set at one hour.

$$Q_{Generic\ profile,t} = \frac{\sum Q_{BuildingX,t}}{\sum Q_{Recorded\ annual,\ BuildingX}} \tag{3.7}$$

This profile is used to determine the hourly heat consumption of buildings for which only data is available with a monthly frequency. The following formula (Equation 3.8) is used to determine the hourly heat consumption. The buildings where this is applicable were indicated by having *Profile* at *Q data frequency* in Table 3.2, which are 9 buildings in total.

$$Q_{Building\ X,\ t} = Q_{Generic\ profile,t} \cdot Q_{Recorded\ annual,\ Building\ X} \tag{3.8}$$

No data available For 11 of the 34 buildings, there is unreliable, insufficient or no data available. Heat data for these buildings is excluded from the analysis. However, based on the real estate developments, the heat demand will decrease by 60 percent from now towards 2030, whereas electricity demand is predicted to remain the same (Province of Utrecht, 2017). Accordingly, it is expected that

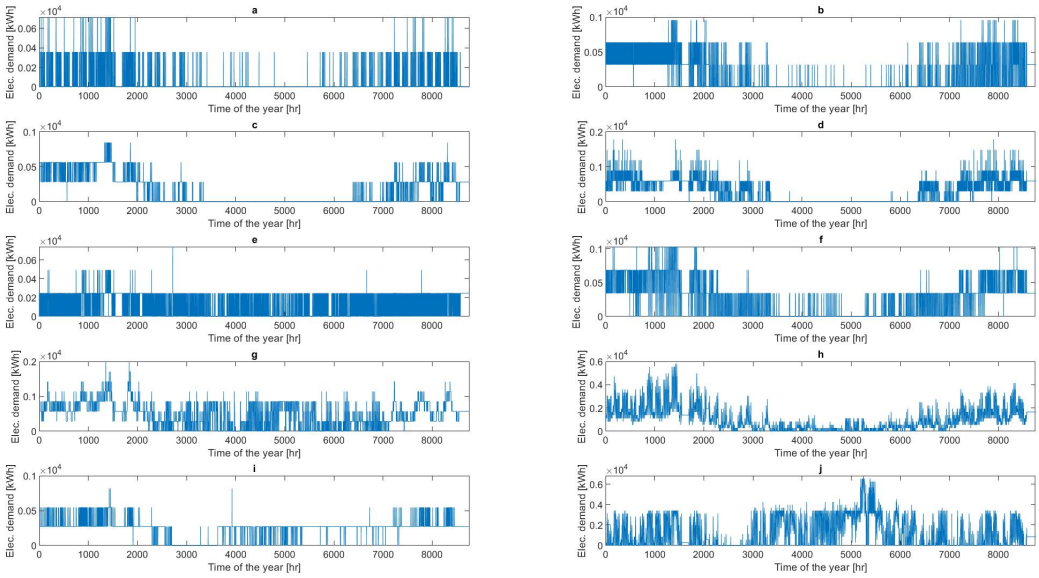

Figure 3.6: Heat demand 10 buildings with an hourly time interval of year 2018, with (a) *01.12 Bleekergeb. (Sorbonnelaan 4)*, (b) *01.23 Ornsteinlab. (Princetonplein 1)*, (c) *01.35 NITG-TNO (Princetonlaan 6)*, (d) *01.52 Buys Ballot lab. (Princetonpl. 5)*, (e) *01.58 Aardwetenschappen (Budapestlaan 4)*, *(f) 02.28 Res.kas+Bot.tuin (Uppsalaln Tuin)*, (g)*02.60 D.de Wiedgeb (Universiteitswg 99)*, (h) *03.77 Hugo Kruytgebouw (Padualaan 8)* (i) *05.27 Univers.Bibliot (Heidelberglaan 3)* and (j) *13.22 Androclusgebouw (Yaleln 1)*.

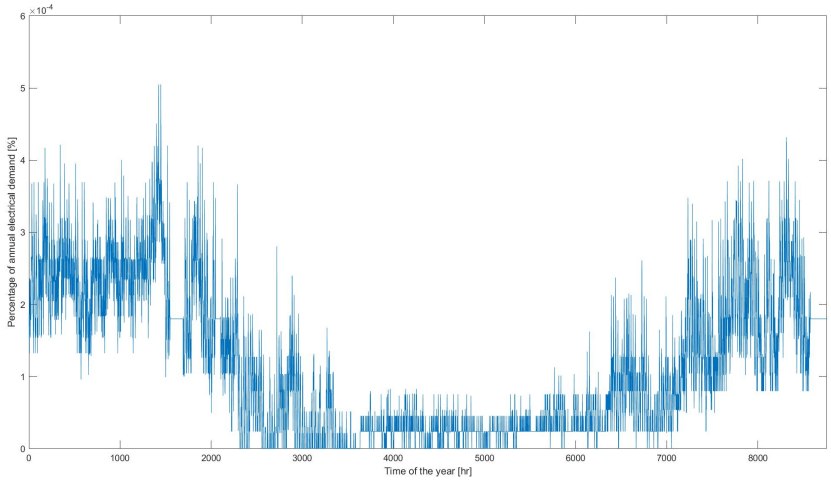

Figure 3.7: Generic heat profile with an hourly time interval, based on; (a) *01.12 Bleekergeb. (Sorbonnelaan 4)*, (b) *01.23 Ornsteinlab. (Princetonplein 1)*, (c) *01.35 NITG-TNO (Princetonlaan 6)*, (d) *01.52 Buys Ballot lab. (Princetonpl. 5)*, (e) *01.58 Aardwetenschappen (Budapestlaan 4)*, *(f) 02.28 Res.kas+Bot.tuin (Uppsalaln Tuin)*, (i) *05.27 Univers.Bibliot (Heidelberglaan 3)*.

the absence of this data would not affect the analysis, since heat demand is expected to decrease over the years.

ATES As mentioned in Section 3.4.2 the operation of the north west ATES system is covered in the total heat demand of the campus. The hourly heat supply by the ATES system is subtracted from the total thermal demand. However, the operation of the system is not properly registered, i.e. only data from January 2018 till August 2018 is available with a monthly frequency. A number of assumptions are made to determine the operational schedule for the months September till December 2018. In general, the months December till March have the lowest outside air temperature, which can be seen in Figure 3.2. Unfortunately, the schedule of December is not available. To overcome this problem, an estimation of the hourly heat supply was made based on the Degree days of December as an fraction ϕ of the Degree days of January till March (Equations 3.9). The degree days per month are determined by a degree day calculator [46]. Based on this fraction and the heat supply in the months January till March the heat supplied in December is estimated. Table 3.4 shows the total heat supply by the system in January till March and the estimated monthly supply in December.

$$\phi_{Degreedays} = DD_{December}/DD_{January-March} = 404.47/1366.53 = 0.2959 \tag{3.9}$$

The hourly supply for December till March is determined based on the monthly supply divided to the amount of hours per month. This amount of heat is subtracted from the hourly demand of the particular building. The hourly supply by the ATES system is assumed to be constant, since the technology's working temperature is low. To provide the buildings with heat during the day, it is assumed that constant heat supply is the most effective way of operation for this system. The hourly supply by the system is presented in Table 3.5.

Table 3.4: The total heat supply by the ATES system in kWh per connected building for the months January till March and the expected heat supply for December of year 2018.

Building	Month	Q ATES system
01.23 Ornsteinlab. (Princetonplein 1)	January - March	121 666 kW h
	December	36 011 kW h
01.35 NITG-TNO (Princetonlaan 6)	January - March	213 333 kW h
	December	63 143 kW h
01.52 Buys Ballot lab. (Princetonpl. 5)	January - March	121 666 kW h
	December	36 011 kW h
01.77 Vening Meineszgebouw A (GEO)	January - March	328 611 kW h
	December	97 263 kW h
01.72 OWC: V. Koningsberger (Budap.ln2)	January - March	531 667 kW h
	December	157 364 kW h

Table 3.5: The expected hourly heat supply by ATES system to connected buildings in kWh of the months January, February, March and December 2018.

Building	January	February	March	December
01.23 Ornsteinlab. (Princetonplein 1)	25.4 kW h	98.4 kW h	49.7 kW h	48.4 kW h
01.35 NITG-TNO (Princetonlaan 6)	63.5 kW h	206.3 kW h	37.0 kW h	84.8 kW h
01.52 Buys Ballot lab. (Princetonpl. 5)	11.57 kW h	107.5 kW h	54.9 kW h	48.5 kW h
01.77 Vening Meineszgebouw A (GEO)	128.1 kW h	222.5 kW h	132.7 kW h	130.7 kW h
01.72 OWC: V.13 Koningsberger (Budap.ln2)	214.7 kW h	346.4 kW h	187.1 kW h	211.7 kW h

In Figure 3.8 the expected total thermal demand of UU is visualised with hourly frequency. This heat profile is used to carry out the analysis.

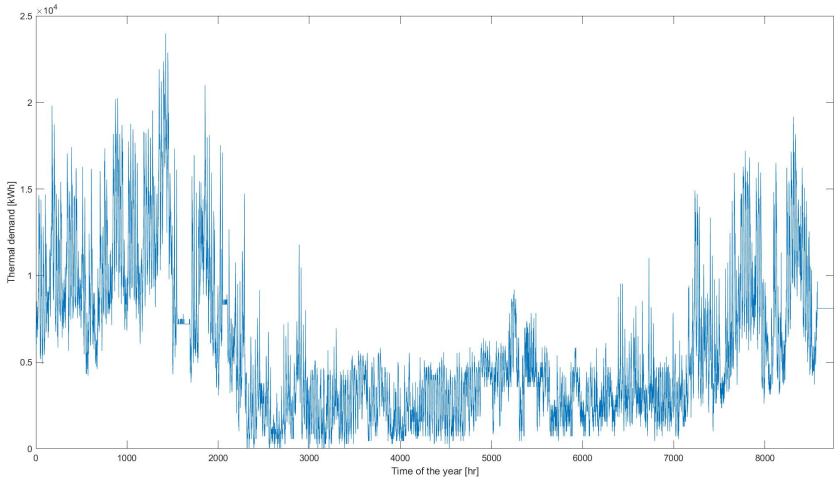

Figure 3.8: Expected thermal demand of UU with an hourly time interval of year 2018. The thermal profile is based on a various number of assumptions, which are discussed in Section 3.4.4

Energy prices and emission factors

Currently, UU imports green gas and electricity. In the future, there might be geothermal heat available according to Pfeiffer (2017) [12]. The next paragraphs exemplify the price and emission factors per carrier.

Electricity UU nowadays consumes green electricity. However, the production of green electricity is not necessarily produced by renewable technologies in the Netherlands. The label 'green' is guaranteed by the GO trading systems. UU wants to be progressive in the local generation of electricity, for this purpose this research considers emission factors for green electricity to create a preference for local generation. The emission factor that is allocated to green electricity is 10 % of the average Dutch emission factor of electricity, which is obtained from CBS (2019) [47].

Gas Above mentioned also applies for the emission factors allocated to the use of natural gas. The import of this green gas is accompanied with an price of $0.192\,\mathrm{EUR\,m^{-2}}$ or $0.0197\,\mathrm{EUR\,kWh^{-1}}$, based on the Dutch upper value for specific heat of gas of $35.17\,\mathrm{MJ\,m^{-3}}$. In addition, UU is buying certificates for greening at $0.11\,\mathrm{EUR\,m^2}$. However, this varies from year to year and is therefore not included in the price. The average Dutch emission factor of gas is obtained from RVO (2017) [48].

Geothermal heat According to Pfeiffer (2017) [12] and Province of Utrecht (2016) [3] there is a potential for extracting geothermal energy in Utrecht. Therefore geothermal heat is also included as an energy carrier for the future. Initial explorations speak of an ultra-deep geothermal, where heat is extracted from the earth at a depth of 7 km [12]. According to Hoogervorst (2017) [49], the cost of supplying deep geothermal heat (depth > 3500 m) is expected to cost around $15.8\,\mathrm{EUR\,GJ^{-1}}$ or $0.057\,\mathrm{EUR\,kWh^{-1}}$. Even though geothermal heat is seen as an energy source with no emission, CO_2 is nevertheless emitted during its extraction. Electricity is used to pump the heated water out of the

Table 3.6: List of the energy prices and emission factors for electricity, geothermal heat and gas. The emission factor of green energy is used during this research, which is based on 10% of the Dutch average emission factor of a particular energy carrier. The presented price and emission factors are allocated to imported energy in the E-Hub tool.

Carrier	Price	Emission factor Green	Emission factor Dutch
Electricity	0.034 - 0.049 EUR kWh^{-1}	$4.50 \cdot 10^{-}05$ tCO_2 kWh^{-1}	$4.50 \cdot 10^{-}04$ tCO_2 kWh^{-1}
Geothermal heat	0.057 EUR kWh^{-1}	$2.25 \cdot 10^{-}06$ tCO_2 kWh^{-1}	$2.25 \cdot 10^{-}05$ tCO_2 kWh^{-1}
Gas	0.020 EUR kWh^{-1}	$1.57 \cdot 10^{-}06$ tCO_2 kWh^{-1}	$1.57 \cdot 10^{-}05$ tCO_2 kWh^{-1}

deeper layers of the soil, which causes CO_2 emissions. The COP of the future geothermal installation is assumed to be 20 [50], the CO_2 emissions related to geothermal heat are expected to be 5% of the Dutch average emission factor of electricity. The energy prices and emissions factors used are presented in Table 3.6 and allocated to imported energy in the E-Hub tool.

3.5 Case Studies

To analyse the opportunities of UU to decarbonise their energy supply, different configurations of energy systems are analysed. The configuration are assessed both on cost and performance in terms of emissions. Two specific cases are selected, UU as end user (I) only wants to decarbonise its electricity supply and (II) it wants to decarbonise their whole energy supply (e.g. electricity and heat supply). This distinction is made to determine the possible benefits if MES is integrated. Considering electricity consumption is expected to remain the same and heat demand probably will decrease towards the year 2030, more value is attached to decarbonising requirements for electricity supply. Both scenarios are subdivided into 2 cases. Figure 3.9 shows a schematic overview of the analysed scenarios and cases, on which next paragraph elaborates. All proposed scenarios are performed using the multi objective optimisation method, which is explained in Chapter 3.3.2. For the proposed scenarios, the optimisations are computed with a gap size of 0.01, using 48 typical days.

I. Decarbonisation of the electricity supply of Utrecht University This scenario examines the importance of Renewable Energy Technologies (RET) such as PV and WT for carbon neutral electricity supply. Since it is yet unknown what kind of storage options are required, this analysis is carried out by use of two sub-scenarios. The first sub-scenario (1) examines the energy system if no seasonal storage option is available (Figure 3.9). The related set of selected technologies are PV, WT and LiB. As second sub-scenario (2), PtG is added in the set of technologies, given its ability to be used as seasonal storage. By making a distinction, the need for seasonal storage can be examined. Both sub-scenarios are investigated with (A) and without (B) the area constraint for wind turbines. Many grasslands are available around the campus, which can potentially be used for installing WTs. In addition, performing both analyses also indicates whether the costs of the analysed system are enhanced due to the area limitations of the campus. Chapter 4 discusses the results of the proposed scenarios.

II. Decarbonisation of the energy provision of Utrecht University The second scenario is based on the design of an MES with an extensive set of technologies that can operate carbon neutral collectively. Therefore the proposed technologies of sub-scenario (2) are extended with ST, edHP, HWTS and boilers (Figure 3.9). The described analysis remains the same. However, this scenario is also divided into two sub-scenarios, namely (3) and (4). Sub-scenario (3) discusses the configured energy system when no geothermal heat import is available, while (4) when it is available. Identical as sub-scenario (1) and (2) are (3) and (4) also examined with (A) and without (B) wind turbine area constraint. For sub-scenario (4) two additional analyses are performed (C) where geothermal heat could be imported accompanied with zero emissions and (D) where the heat is supplied with zero emission and at low cost ($6\,\mathrm{EUR\,GJ^{-1}}$), this to determine whether this accelerates the gas substitution.

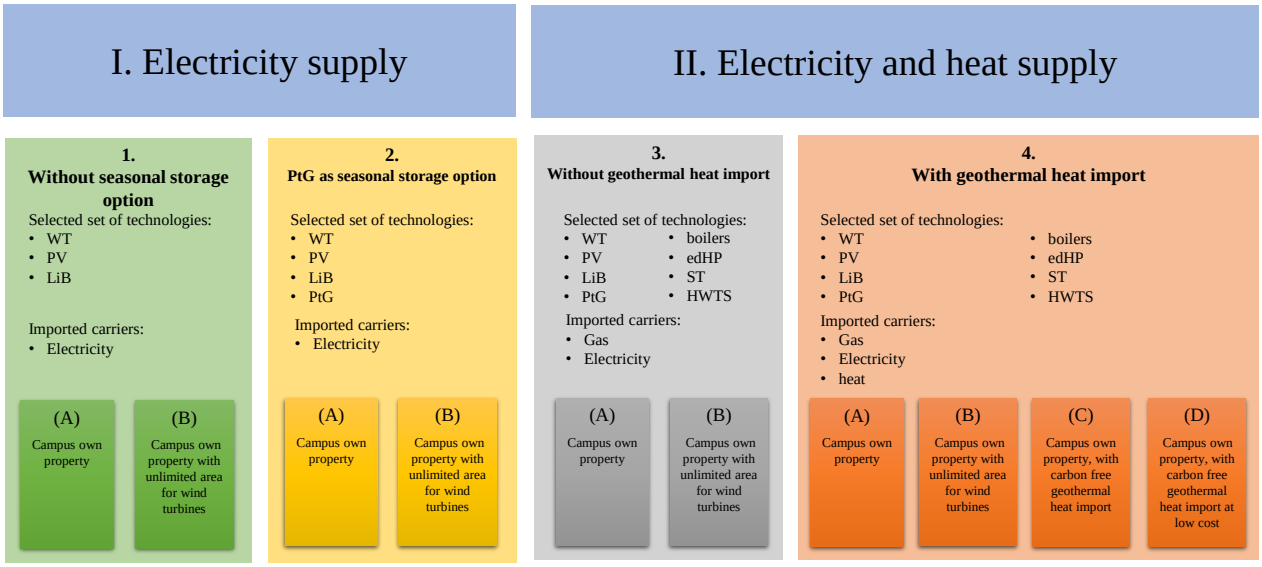

Figure 3.9: Schematic overview of the proposed scenarios and cases. (I) represents scenario one where UU only is an end user of electricity, where (II) represents the scenario where UU wants to decarbonise their whole energy supply. Scenario (I) is subdivided in two sub-scenarios (1) and (2). Sub-scenario (1) examines the energy system if no seasonal storage option is available and (2) when PtG is added in the set of technologies. Both sub-scenarios are investigated with (A) and without (B) wind turbine area constraint. Scenario (II) is also subdivided in sub-scenarios (3) and (4), at which (3) discusses the multi energy system if no geothermal heat is available and (4) if geothermal heat import is allowed. Identical as (1) and (2) are (3) and (4) also examined with (A) and without (B) wind turbine area constraint. For sub-scenario (4) two additional analyses are performed (C) where geothermal heat could be imported accompanied with zero emissions and (D) where geothermal heat could be imported at low cost accompanied with zero emissions.

Chapter 4

Results I - Electricity supply

Decarbonisation of the electricity supply of Utrecht University

4.1 Levels of decarbonisation

In the following, the design of an energy system is discussed per emission reduction achieved. The analysis is performed at which the input data and constraints relevant to the campus are arranged to one node. This section discusses scenario 1A and 1B of Figure 3.9. The selected technologies for the optimisation are (i) PV panels, (ii) WTs and (iii) LiBs. As energy carrier, only electricity is selected. The Pareto front in Figure 4.1 shows the related electricity price, total annual costs and emission reduction achieved by the design. Table 4.1 presents the relative cost increase per emission reduction.

4.1.1 Invest to decarbonise

As expected, the costs for decarbonised electricity is significantly higher in case (1A) significant higher than in case (1B) (Figure 4.1). Which indicates that the campus area is not spacious enough. Due to the larger share of PV, more LiB investment is required in situation (1A) compared to (1B). A remarkable observation is that the costs for the designs for more than 90% emission reduction increase enormously in both cases. This is probably due to the absence of a seasonal storage technology in the set of technologies. From an economic perspective, the costs for CO_2 reduction are extremely high, since above 30% reduction in scenario (1A) the electricity price is more than doubled (Table 4.1). The targeted level of decarbonisation is set at 80 - 95 % reduction by 2030. However, cost for this configuration of the design is probably financially infeasible, given that the electricity price increases by a factor of at least six for this emission reduction.

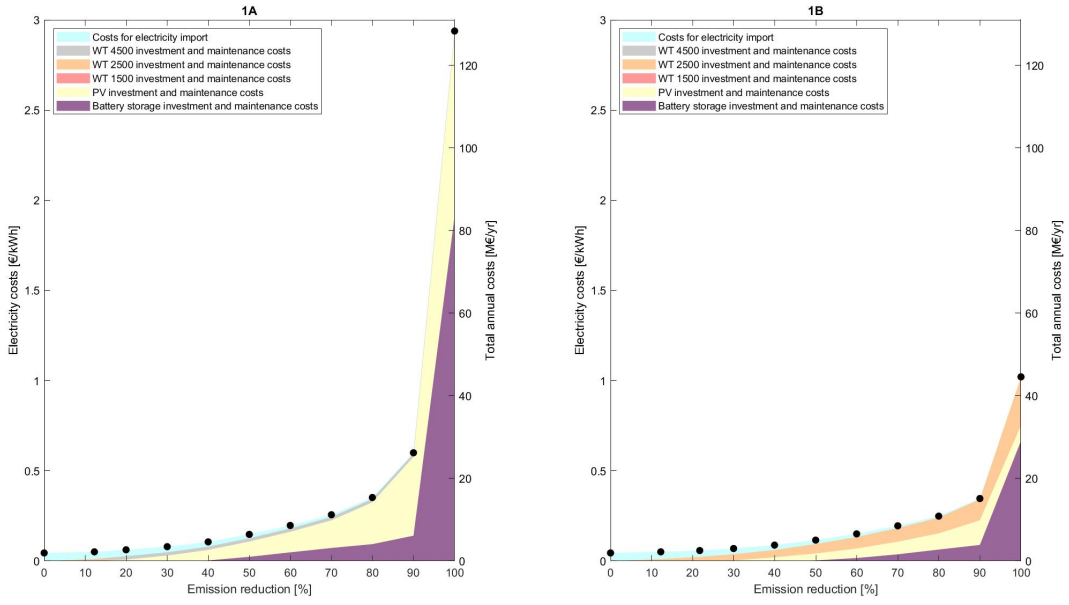

Figure 4.1: Cost-emission Pareto front for sub-scenario 1 for electricity supply to UU with as available set of technologies; WTs, PV panels, and LiB for (1A) the campus property (1B) campus property with unlimited area for WTs. In this scenario only electricity import is allowed.

Table 4.1: Relative cost increase per emission reduction achieved by the design compared to reference for scenario (1A) campus area and (1B) campus area with unlimited area for WTs. The bold value indicates the maximum emission reduction that can be achieved if electricity costs are not more than doubled.

CO_2 reduction	Relative cost increase (1A) [%]	Relative cost increase (1B) [%]
Reference	-	-
10 %	13.5 %	13.5 %
20 %	39,0 %	29.7 %
30 %	**77,5** %	54.7 %
40 %	136,3 %	**96.4** %
50 %	229,0 %	158.2 %
60 %	339.3 %	235.5 %
70 %	471.4 %	334.7 %
80 %	683.9 %	454.1 %
90 %	1235.7 %	670.9 %
100 %	6437.3 %	2172.1 %

4.1.2 Technology sizes

The capacities of the installed technologies along the Pareto front are plotted for situation (1A) and (1B) (Figure 4.2). A number of considerations are made based on this figure. In none of the designs WTs of 1500 kW are installed, as well for scenario 1A as 1B (Figure 4.2(d)). Different combinations of WTs and PV panels are present in the designs to satisfy electricity demand. At low emission reductions, WTs are more preferred than PV panels in the configurations of the optimal designs. A maximum of two WTs of 4500 kW can be installed at the available area, while 2500 kW are more favourable in case no area constraint for WTs is implemented. This is noticeable by the fact that in scenario (1A) two WTs of 4500 kW are installed, while in (1B) 46 units of 2500 kW are installed when fully decarbonising the electricity supply. This preference can possibly be caused by the occurrence that the cut in and cut out speed matches better with the wind speeds at the campus. Another important result is that in scenario (1B) the total area available for PV, even when the energy system is fully decarbonised, is not entirely utilised. Indicating yet again that the investment in WTs is more cost effective for UU electricity supply. This is probably caused by the the seasonal and day to day variation in PV panel output, which requires more electricity import. Section 4.1.3 elaborates on this occurrence. With regard to investment in storage options, at 90% reduction Figure 4.2(e) shows an extremely high increase in capacity. From this it can be assumed that from this point the system requires seasonal storage. To support this assumption, the energy stored during the year needed to be analysed.

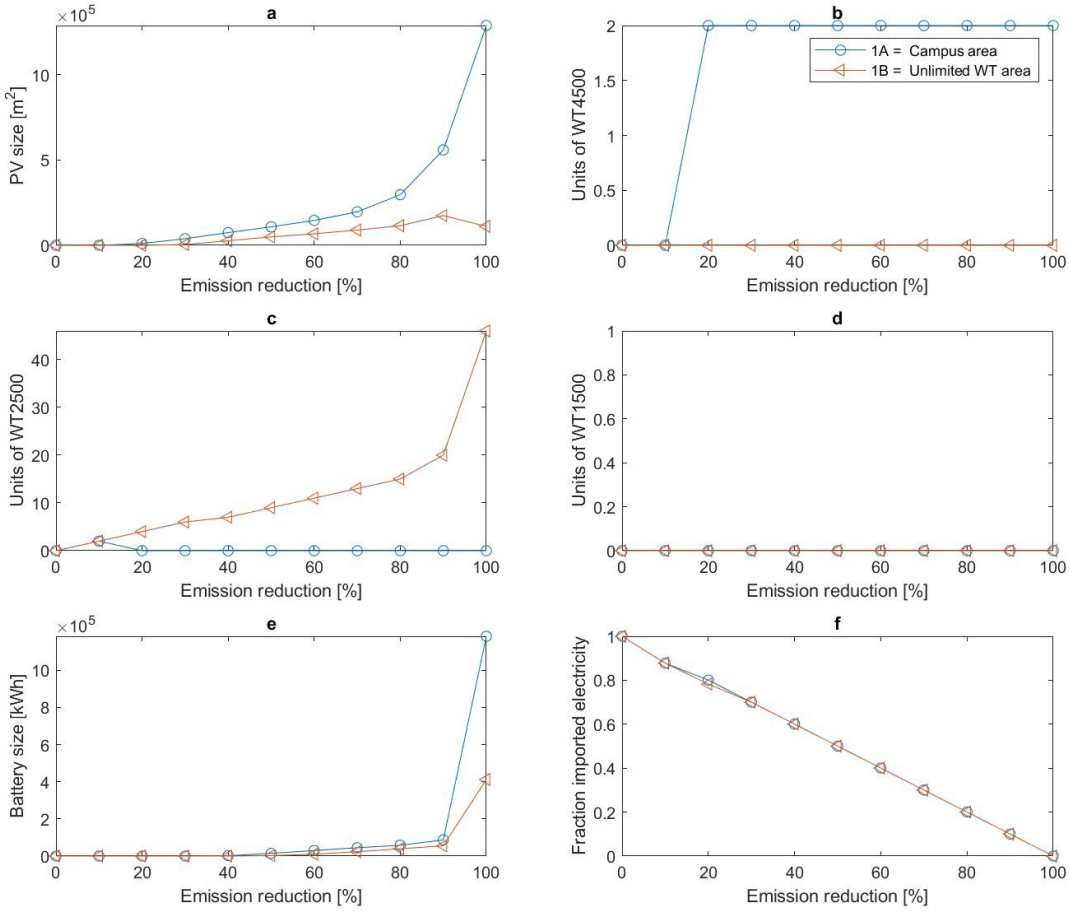

Figure 4.2: Size of the installed technologies along the Pareto fronts for scenario 1A (blue circle) and 1B (orange triangle): (a) PV panels, (b) 4500 kW WTs, (c) 2500 kW WTs, (d) 1500 kW WTs, (e) LiBs. Graph (f) shows the amount of imported electricity as a fraction of the total electricity demand.

4.1.3 Technology outputs

To get an indication of how the electrical power of the technologies relates to the electricity demand, the output per technology with an hourly frequency is presented in Figure 4.3 & 4.4, for scenario 1A and 1B respectively. In this case the electrical surplus can be seen as the energy stored at a later point, which is also clearly visible by the battery output due to discharging just after the surplus. When observing the differences between both figures, the generation scenario 1B corresponded in scenario 1A, since there were less peaks above demand observed. PV has an extremely varying output, while the WT output is more constant. This confirms the previously noted preference for WTs rather than PV.

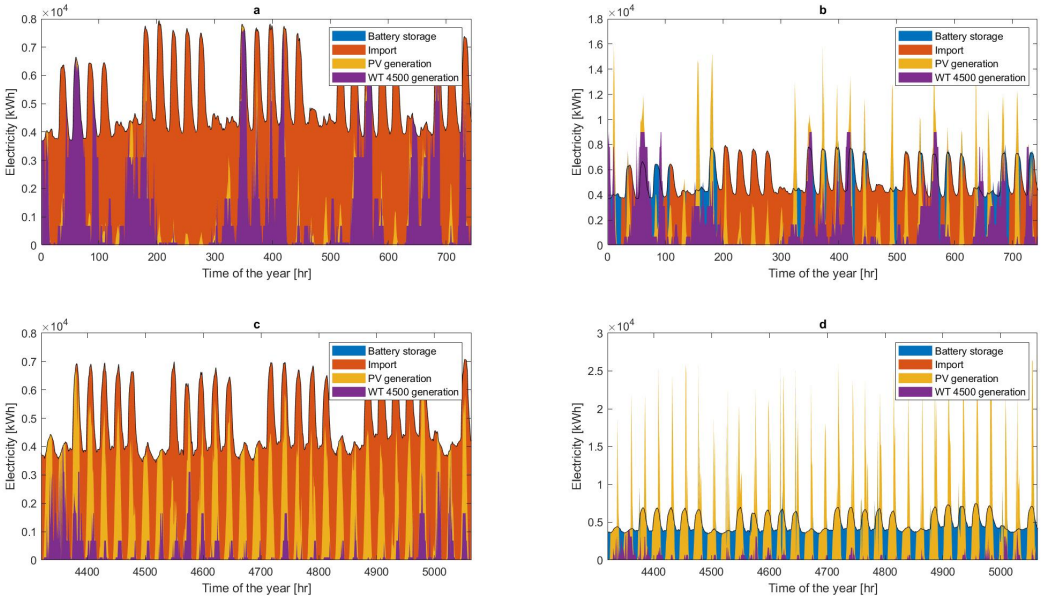

Figure 4.3: Electrical output of the technologies that were included in the optimal design of scenario 1A for (a) in January and (c) in July for 30 % emission reduction and (b) in January and (d) in July for 80% emission reduction.

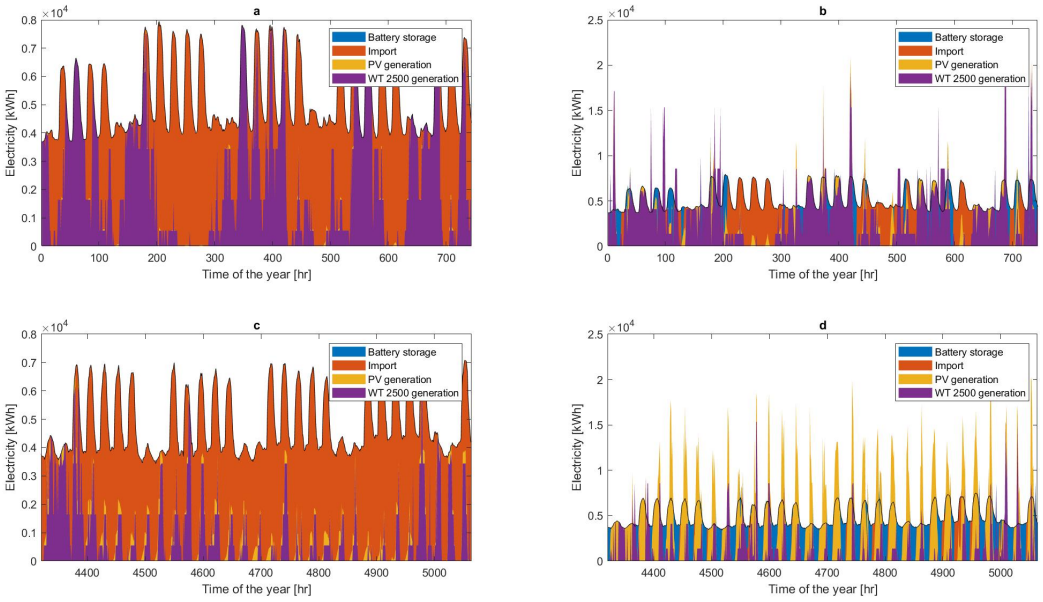

Figure 4.4: Electrical output of the technologies that were included in the optimal design of scenario 1B for (a) in January and (c) in July for 30 % emission reduction and (b) in January and (d) in July for 80 % emission reduction.

4.1.4 Storage

Figure 4.5 shows the hourly electricity stored by the LiB. Given that at the designs with lower emission reductions no battery is used, the battery output of the designs with higher emission reductions is

discussed, in this case 80 % and 100% reduction. The electricity stored in the LiB at 80% shows an increase in the summer and decrease in winter (Figure 4.5 1A(b)), while at 100% (Figure 4.5 1A(c)) shows an decrease towards summer and an extreme increase towards winter, where at the end of the year the battery is totally discharged. This result confirms the earlier assumption of the need of seasonal storage. In Figure 4.5 1A(b) the influence of the sun on the generated power is clearly visible. During summer there is a surplus and the battery is charged while in winter the battery is almost only discharging. When looking at the energy stored in the battery for scenario 1B, Figure 4.5 1B(b) shows less seasonal variability, since more WTs are present in this design. In addition, in this scenario there is less need for seasonal storage, since in Figure 4.5 1B(c) no seasonal pattern is seen in the energy stored. Considering the explicit need of seasonal storage in scenario 1A, PtG is added to the set of technologies, on which the next section elaborates.

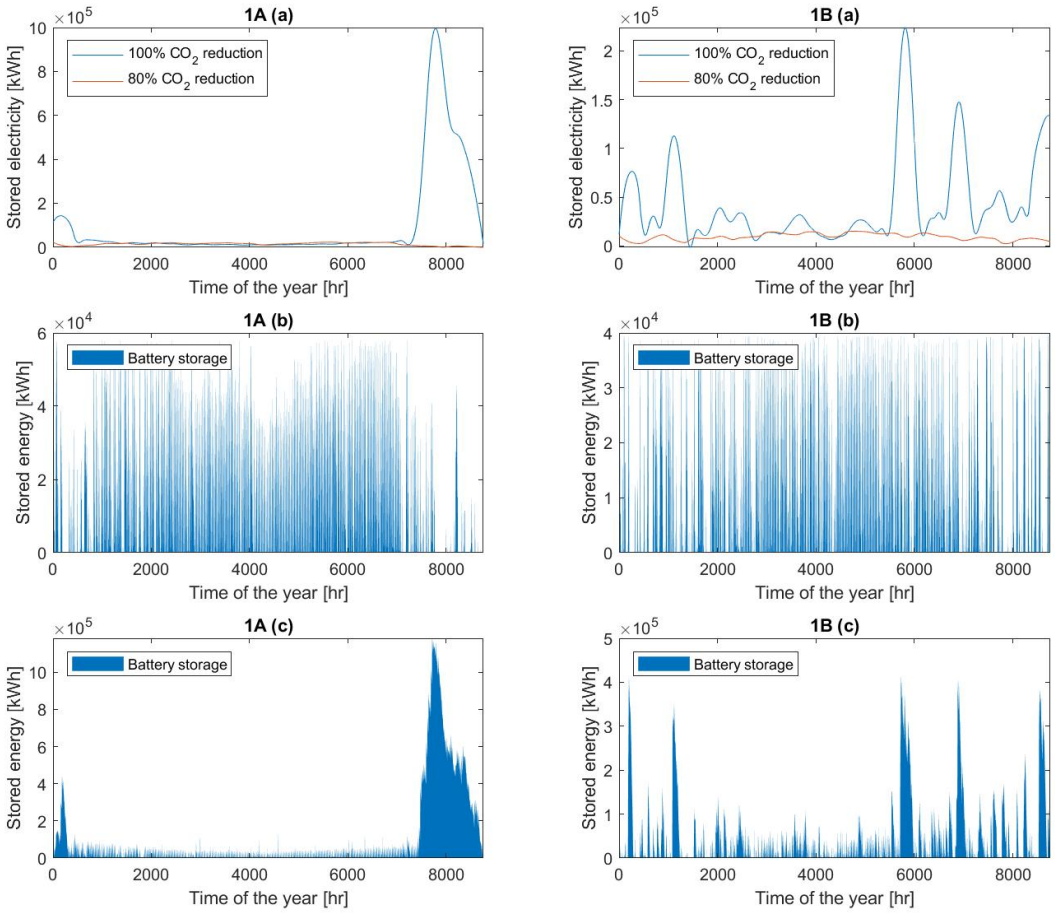

Figure 4.5: Amount of electricity stored over the year divided in scenario 1A and 1B, where Graph (a) represents the electricity stored for the 100% emission reduction and 80% emission reduction. The hourly electricity stored is based on the loess regression, which uses a local weighted regression to fit a smooth curve through the points, allowing to reveal trends and cycles of the electricity stored throughout the year. Graph (b) shows the battery storage for designs with 80% and (c) for 100% emission reduction.

4.2 Introducing Power To Gas

This section examines sub-scenario 2 of Figure 3.9. To determine at which of the designs along the Pareto front UU should invest in seasonal storage, the PtG technology is included in the set of technologies, consisting of PEMEC, HOS and PEMFC. This analysis is performed under the same conditions as the run in the previous section except hydrogen is added to the set of energy carriers.

4.2.1 Effect of introduction of PtG on the cost and size of technologies

From Figure 4.6 conclusions can be drawn that only above 80% emission reduction, where total electricity supply is divided into 20 % import and 80% local generated electricity, it is necessary to look at options for seasonal storage of electricity, considering that from this point on the system invests in PtG.

4.2.2 Cost and size influence due Power to Gas

Comparing Table 4.1 and 4.2 the price increase is influenced positively for scenario (2A) above the 90 % and for (2B) 100% emission reduction. For the remaining levels, the values correspond to the previous analysis with LiBs as only storage option. Small differences are probably caused by the GAP size. In Figure 4.7(g) and (h) at the 50% and 60% emission reduction of (2A) the design contains PEMEC with small capacities of PEMFC and HOS, which are not visible due to the large scale needed for the capacities needed in the designs of with higher emission reductions. The higher capacity of PEMEC is probably caused by presence of the high amount of PV. When looking at

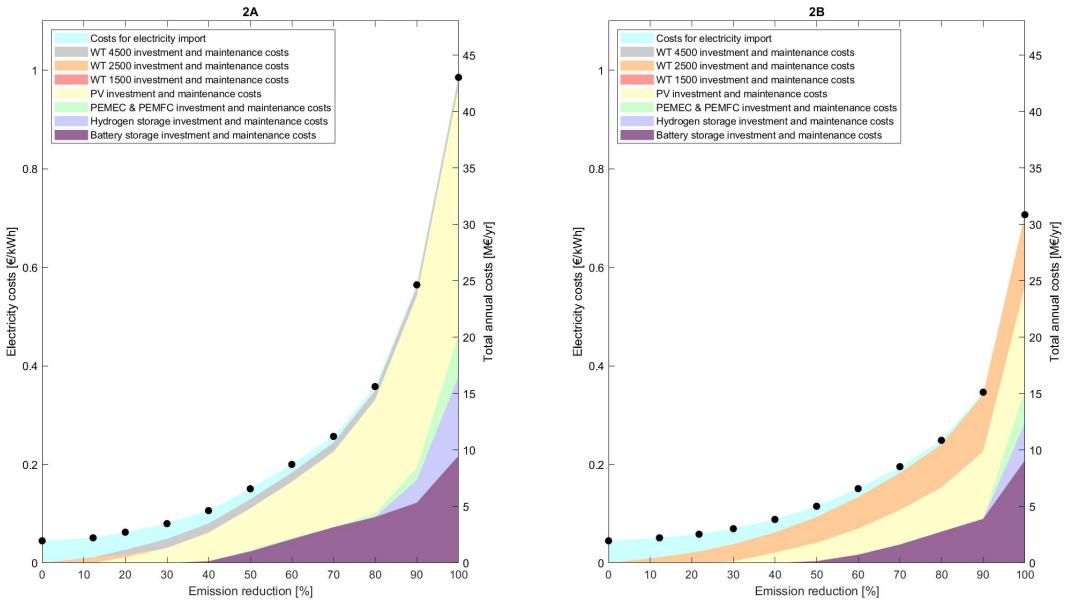

Figure 4.6: Cost-emission Pareto front for sub-scenario 2 for electricity supply to UU with as available set of technologies; WTs, PV panels, LiB and PtG for (2A) the campus property (2B) campus property with unlimited area for WTs. In this scenario only electricity import is allowed.

Table 4.2: Relative cost increase per emission reduction achieved by the design compared to reference for scenario (2A) campus area and (2B) campus area with unlimited area for WTs. The bold value indicates the maximum emission reduction that can be achieved if electricity costs are not more than doubled.

CO_2 reduction	Relative cost increase (2A) [%]	Relative cost increase (2B) [%]
Reference	-	-
10 %	13.5%	13.5 %
20 %	38.8%	29.7 %
30 %	**77.5%**	54.7 %
40 %	136.3 %	**96.4** %
50 %	234.9 %	156.0 %
60 %	345.1 %	235.5 %
70 %	471.4 %	334.7 %
80 %	696.5 %	453.6 %
90 %	1155.8 %	670.9 %
100 %	2092.5 %	1472.3 %

the sizes of the installed technologies in Figure 4.7(e)(f) less WTs are installed and LiB capacity decreased considerably compared to installed capacities in the designs of scenario 1A and 1B (Figure 4.2). In this case it is more cost effective to install a larger capacity of HOS storage than to increase the capacity of WTs to ensure electricity supply in winters. Seasonal compensation for renewable electricity generation is necessary for designs with emission reductions above 80% in scenario 2A and for scenario 2B above 90% reduction.

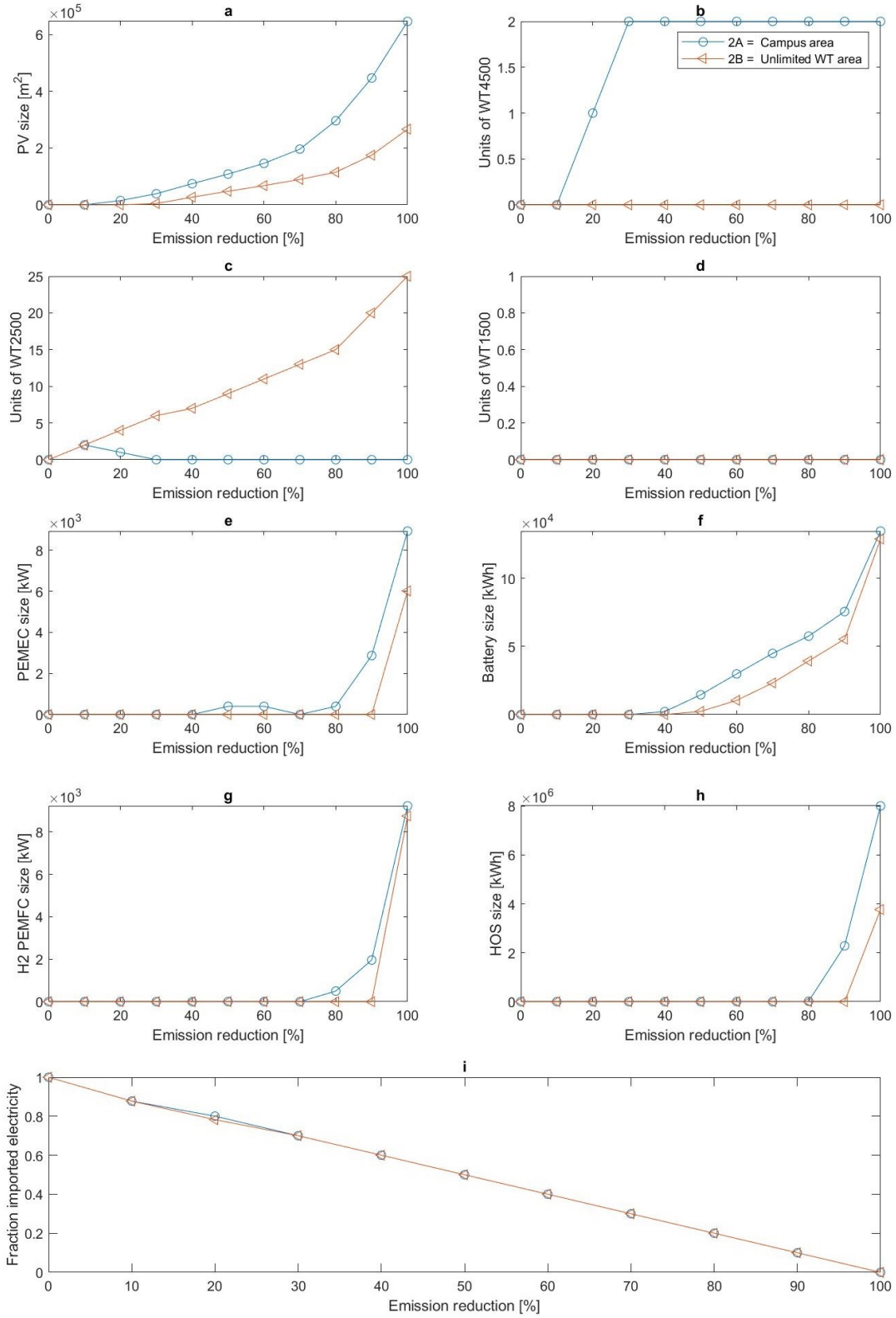

Figure 4.7: Size of the installed technologies along the Pareto fronts for scenario 2A (blue circle) and 2B (orange triangle):(a) PV panels, (b) WT 4500, (c) WT 2500, (d) WT 1500, (e) PEMEC (f) Battery (g) H_2 PEMFC and (h) HOS. Figure (i) shows the amount of imported electricity as a fraction of the total demanded electricity.

4.2.3 Storage distribution

To investigate how the electricity generation during the year is distributed over the two storage options the energy stored is plotted with an hourly frequency (Figure 4.8). Since for the designs with lower emission reductions little or no hydrogen storage is required, only the storage distribution of the storage technologies in the designs with 90% and 100% emission reduction are discussed. In addition, the stored energy is subdivided into LiB storage and HOS storage. When the system operates fully renewable (maximum decarbonisation) three times as much energy is stored towards the end of the year compared 90% reduction. With respect to the characteristics of these storage options, the LiB is utilised as day to day storage option (short cycles), while PtG is used as seasonal storage option, given its seasonal cycles. It is worth noticing that with in scenario 2B seasonal storage is only required in case of full decarbonisation (Figure 4.8(b)(c)).

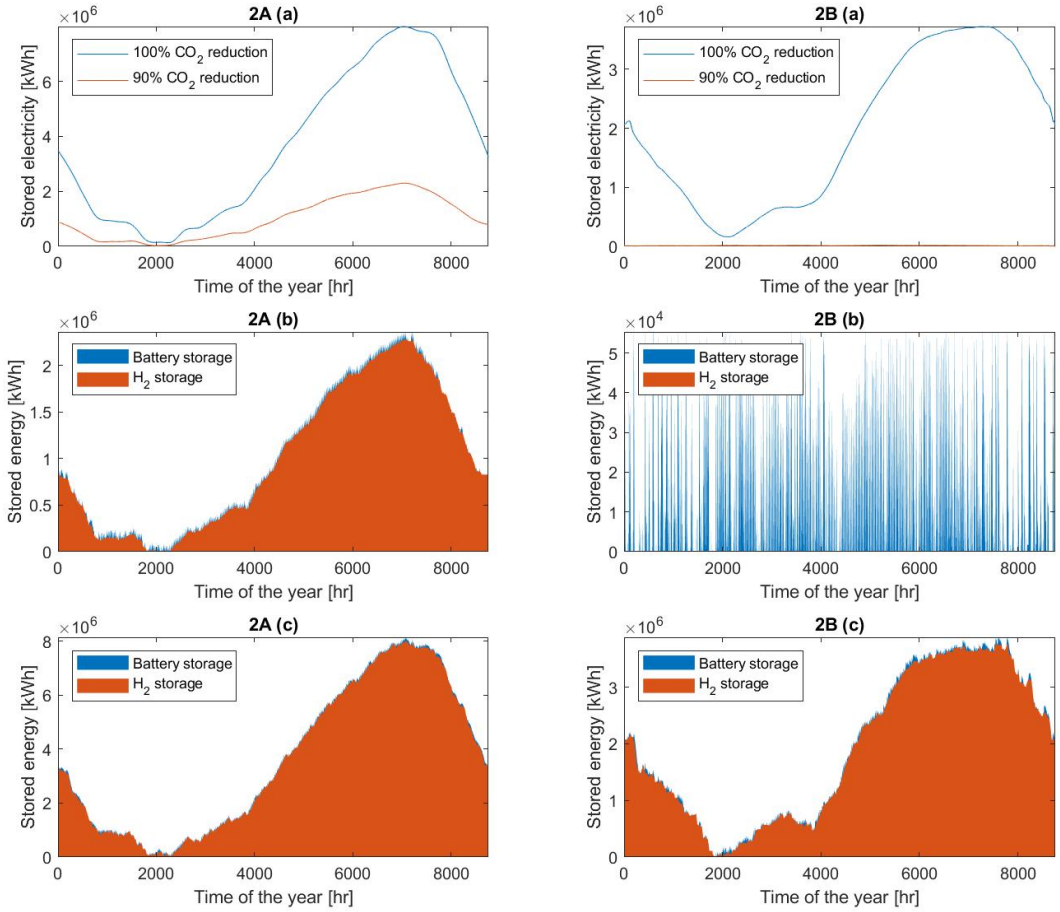

Figure 4.8: Amount of electricity stored over the year divided in scenario 2A and 2B, where Graph (a) represents the electricity stored for 100% emission reduction and 90% emission reduction. The hourly electricity stored is based on the loess regression, which uses a local weighted regression to fit a smooth curve through the points, allowing to reveal trends and cycles of the electricity stored throughout the year. Graph (b) shows the electricity stored divided in the different energy carriers for designs with 90% and (c) for 100% emission reduction.

Chapter 5

Results II - Electricity and heat supply

Decarbonisation of the energy provision of Utrecht University

5.1 Multi energy system approach

To asses whether the MES approach is more cost effective, but above all to indicate whether it is possible to supply decarbonised heat and electricity with the available area at the campus, the optimisation is performed under the same conditions as described in Section 4.1, but heat-producing and storage technologies are added and the set of energy carriers are expanded. This section discusses scenario 3A and 3B (Section 3.5). In the optimisation import of electricity and gas is possible. If the installed capacities of the existing edHPs and boilers in the designs of UU do not exceed the existing capacities, their presence is not reflected in the Pareto front, since there are no investment costs allocated to the existing technologies. Figure 5.1 presents the Pareto front for the optimised MESs.

5.1.1 Feasibility of local generation of heat and electricity

In scenario (3A), the analysed MES could not reach full decarbonisation due to the area limitation. The maximum CO_2 reduction achieved is 99.48 %, which indicates that it is infeasible to create a fully renewable energy system with available land at the campus. Upwards to 80% reduction there is mainly invested in renewable electricity conversion or storage technologies. This occurrence is probably caused due to; (i) higher CO_2 emission rate of electricity, (ii) the existing heat pumps and boilers, (iii) the more affordable price of WT and PV compared to ST and HWTS and (iv) the absence of a seasonal storage technologies which has a thermal energy input instead of electrical. Table 5.1 shows the relative cost increase per emission reduction. At the designs with low emission reductions, the

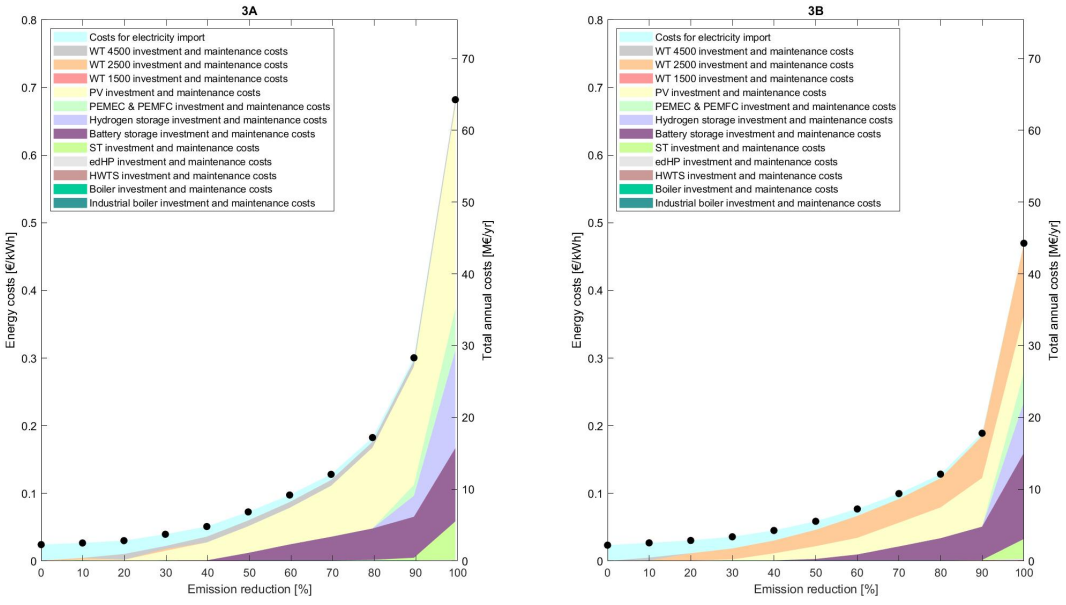

Figure 5.1: Cost-emission Pareto front for sub-scenario 3 for electricity and heat supply to UU with as available set of technologies; WTs, PV panels, LiB, PtG, edHP, boilers, industrial boilers, ST and HWTS for (3A) the campus property (3B) campus property with unlimited area for WTs. In this scenario only import of electricity and gas is allowed.

Table 5.1: Relative cost increase per emission reduction achieved by the design compared to reference level for scenario (3A) campus area and (3B) campus area with unlimited area for WTs. The bold value indicates the maximum emission reduction that can be achieved if electricity costs are not more than doubled.

Emission reduction	Relative cost increase (3A) [%]	Relative cost increase (3B) [%]
Reference	-	-
10 %	10.2 %	14.5 %
20 %	24.3 %	29.7 %
30 %	**63.1 %**	52.7 %
40 %	110.8 %	**92.3 %**
50 %	200.1 %	150.2 %
60 %	303.4 %	227.8 %
70 %	430.0 %	324.6 %
80 %	655.1 %	446.9 %
90 %	1143.1 %	704.5 %
100 %	– %	1900.2 %

cost increase of the system is higher in scenario 3B than in 3A, which is an unusual outcome for which no explanation has yet been found. However, from that point onward the cost increase of 3B is lower than 3A.

5.1.2 Technology sizes

Figures 5.2 and 5.3 represent the sizes of technologies installed for the Pareto optimal designs. Figure 5.2 shows again the preference for WTs rather than PV. Comparing the installed units of 2500 kW WTs and 4500 kW WTs, 2500 kW WTs are yet again preferred in the configurations. Electricity production technologies are increased in the configurations, while the existing heat technologies capacities remain equal. This indicates that the substitution of electricity import is most cost effective to achieve decarbonisation. Above 90 % emission reduction, the capacities of edHPs increase along with installed capacities of electricity generating technologies, which indicates electrification of heat.

Figure 5.2(h) shows that in the designs in general in scenario 3A the capacities of the existing edHPs are not fully utilised. This is probably caused due to the area limitation for WTs, since this is not the case for scenario 3B. A cheaper option is to use gas and invest in additional boilers rather than to invest in PV and storage or electricity import to run the heat pumps. When the area for WT is limited, the electricity production is mainly used for electricity purposes instead of heat production. This assumption is based on utilisation of the edHP. For the limited area, the existing edHP capacity is not fully utilised, while its full capacity is utilised when more WTs can be installed. There is overall mainly invested in electricity production technologies rather heat production. Therefore investment in electrical storage technologies (e.g. LiB) is favoured compared to heat storage technologies (e.g. HWTS) (Figure 5.3. ST becomes important at when higher emission reduction wants to be achieved and is accompanied by high capacities of HWTS. A main disadvantage of ST is its dependency of the sun. The operational output of ST is at highest in summer, while demand is highest in winters. Therefore high capacities must be installed in order to be able to provide enough heat during winter.

At the reference point, the ratio between electricity and gas import is nearly equal. Comparing the fractions of energy import and CO_2 emission reduction (Figure 5.3), it becomes obvious that electricity import has the highest impact, since at lower emission reduction electricity import is substituted by PV and WT installation, while heat generation technologies remained almost the same in capacity.

Moreover, the dissimilarity in the CO_2 emission rates for gas and electricity is clearly visible, since the slope of the gas fraction much steeper per emission reduction. High capacities of batteries are necessary through the high amount of PV and WT. In case of absence of ST in the configured designs, the investment in HWTS is lesser of interest. Given the presence of multiple storage technologies for the for designs with high emission reductions, the following section elaborates on the distribution of the storage for the different energy carriers.

5.1.3 Storage distribution

Considering that three different storage options are deployed in designs with higher emission reductions than 80%, the energy stored along the year is plotted for 80% en 100 % emission reduction, which is presented in Figure 5.4(a). Additionally, a distinction is made in the distribution of storage over the different energy carriers (i.e. heat, electrical, hydrogen storage) (Figure 5.4(b)(c)) Thermal storage and battery storage compensates the short therm mismatches caused by renewable energy generation, while the operation of the PtG provides energy for the seasonal mismatch. In case the wind area is not limited, considerably less ST is installed since the electricity produced by the WT could be used for operation of the existing edHPs and therefore at 90% reduction the design does not require a seasonal storage option. The nature of the different storage options (e.g. day to day or seasonal) is clearly reflected in the cycles.

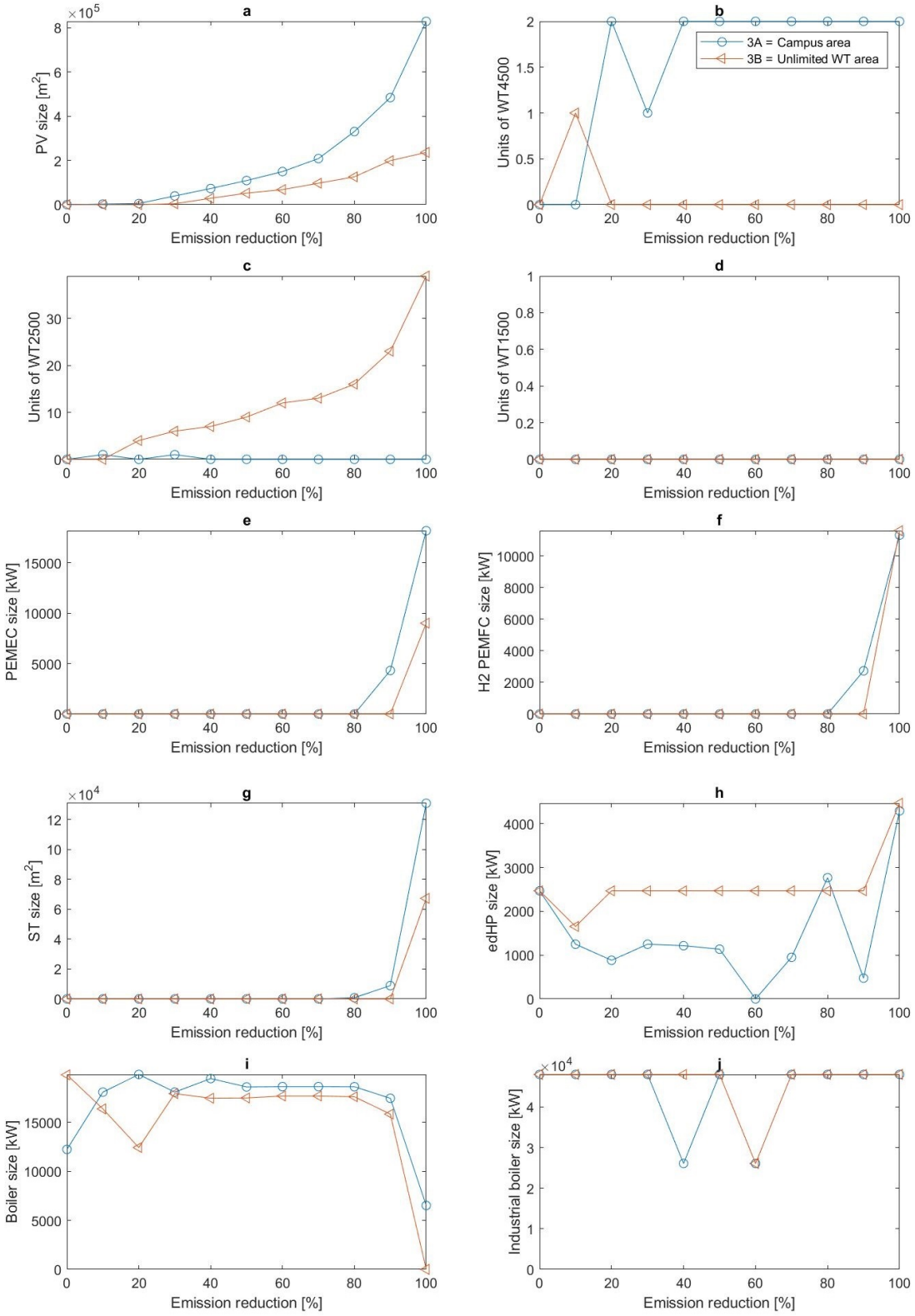

Figure 5.2: Size of the installed technologies along the Pareto fronts for scenario 3A (blue circle) and 3B (orange triangle):(a) PV panels, (b) WT 4500, (c) WT 2500, (d) WT 1500, (e) PEMEC and (f) H_2 PEMFC, (g) ST panels, (h) edHPs, (i) boilers and (j) industrial boilers.

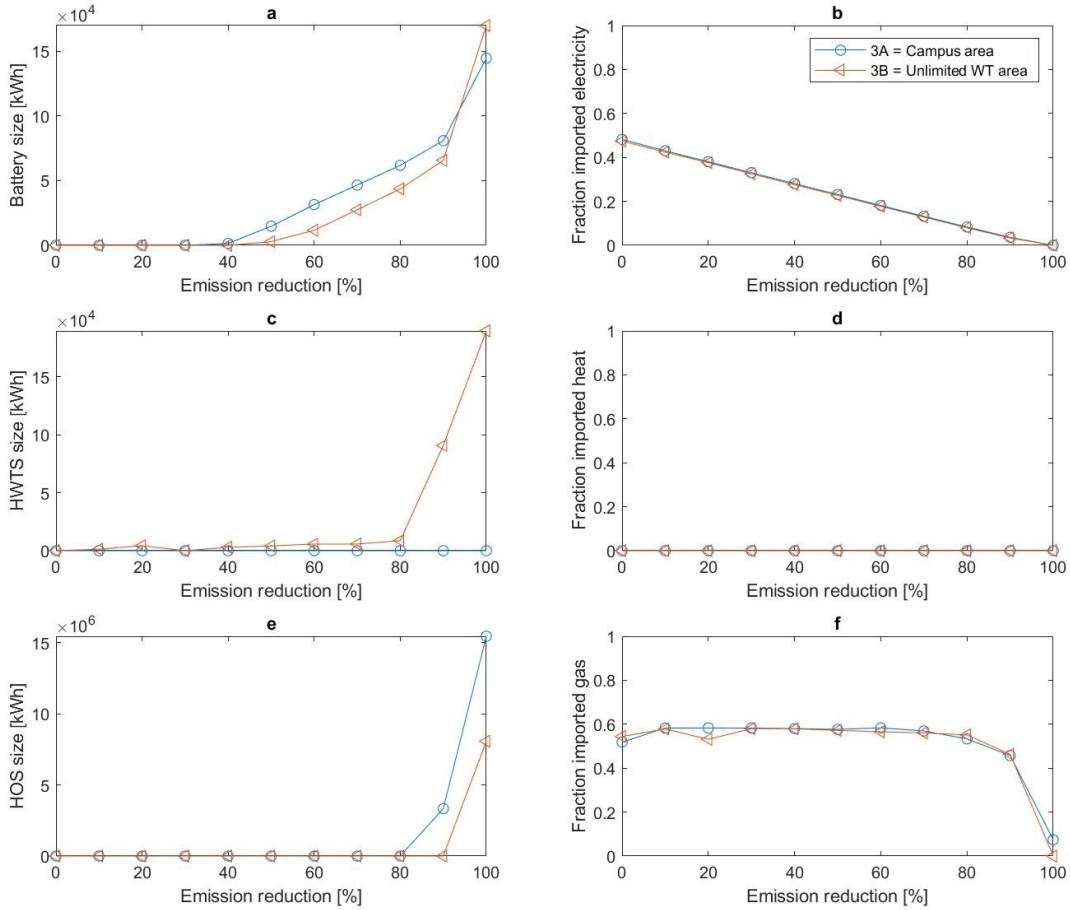

Figure 5.3: Size of the installed technologies along the Pareto fronts for scenario 3A (blue circle) and 3B (orange triangle): (a) Battery, (c) HWTS and (e) HOS. Graph (b), (d), (f) represent the fraction imported electricity, heat and gas of the total energy demand.

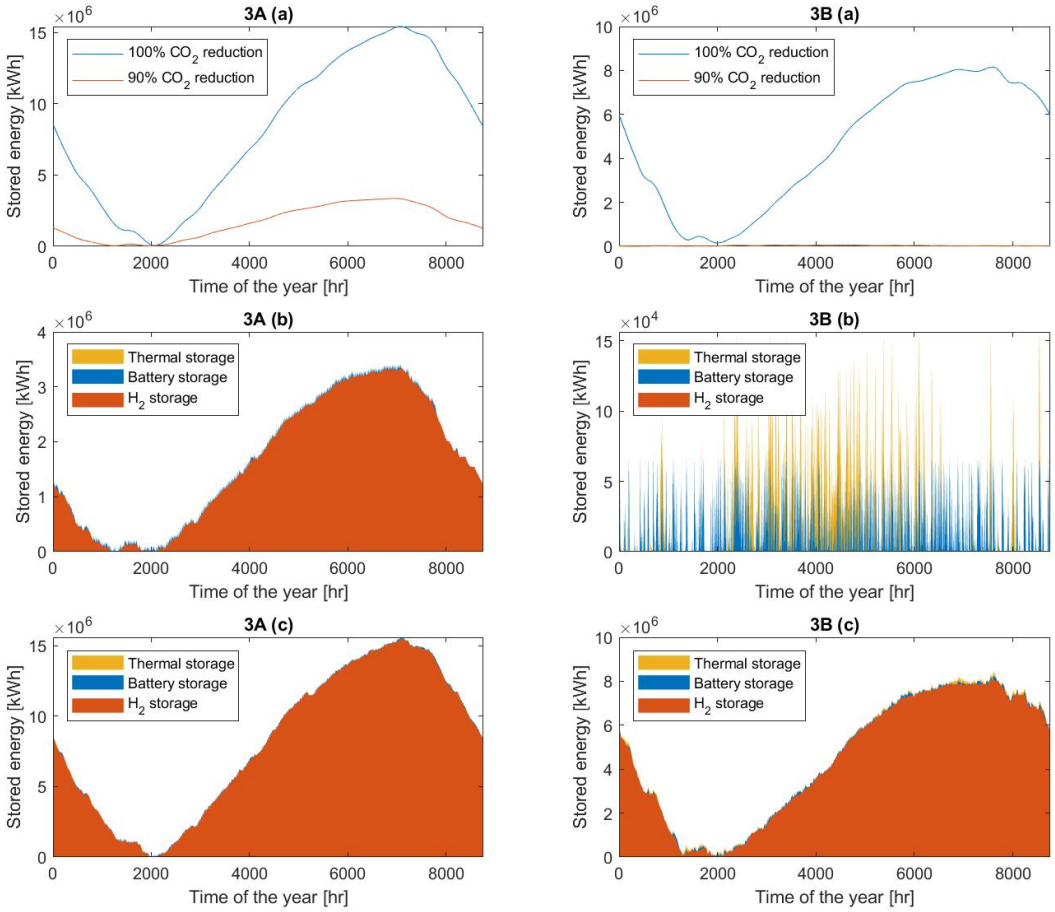

Figure 5.4: Amount of energy stored over the year divided in scenario 3A and 3B, where Graph (a) represents the energy stored for 100% emission reduction and 90% emission reduction. The hourly energy stored is based on the loess regression, which uses a local weighted regression to fit a smooth curve through the points, allowing to reveal trends and cycles of the energy stored throughout the year. Graph (b) shows the energy stored divided in the different energy carriers for designs with 90% and (c) for 100% emission reduction.

5.2 Introducing Geothermal heat

To indicate whether it offers advantages to UU to participate in the geothermal project, this scenario is performed with the possibility of heat import. Taking in mind UU network has not been connected to any external heat network, additional costs have to be taken into account when considering this connection.

5.2.1 Impacts on the configuration and operation of the system

Figure 5.5 presents the Pareto front of the analysed system. Comparing (4A) of this Pareto front with the Pareto front of scenario (3A) (Figure 5.1, it seems that costs have been decreased for the highest achievable decarbonisation. However, this is actually not the case since a lower maximum emission reduction is reached, namely 99.39 %. This small change is probably caused by the gap size.

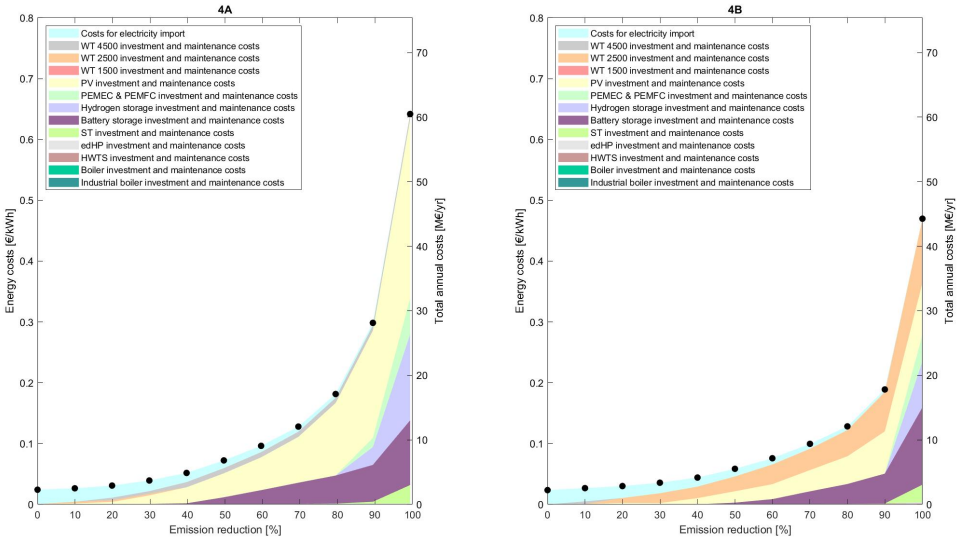

Figure 5.5: Cost-emission Pareto front for sub-scenario 4 for electricity and heat supply to UU with as available set of technologies; WTs, PV, LiB, PtG, edHP, boilers, industrial boilers, ST and HWTS for (4A) the campus property (4B) campus property with unlimited area for WTs. In this scenario import of electricity, geothermal heat and gas is allowed.

Table 5.2: Relative cost increase per emission reduction achieved by the design compared to reference for scenario (4A) campus area and (4B) campus area with unlimited area for WTs. The bold value indicates the maximum emission reduction that can be achieved if electricity costs are not more than doubled.

CO_2 emission reduction	Relative cost increase (4A) [%]	Relative cost increase (4B) [%]
Reference	-	-
10 %	9.6 %	13.9 %
20 %	28.2 %	28.3 %
30 %	**62.9 %**	51.7 %
40 %	114.0 %	**87.8** %
50 %	199.0 %	149.0 %
60 %	298.1 %	222.7 %
70 %	428.9 %	323.5 %
80 %	650.5 %	445.7 %
90 %	1134.2 %	703.6 %
100 %	– %	1897.7 %

Despite the comparable Pareto fronts of sub-scenario 3 and 4, there are some minor changes in the system's configuration. Comparing Figure 5.6 with 5.2 and Figure 5.7 with 5.3 the following is noted; namely; (i) at 20 % decarbonisation the configuration of 4A contains one WT less (Figure 5.6) than in 3A, (ii) boiler sizes are slightly decreased and the (iii) capacities of heat pumps vary along the pareto points. Although the impacts are small, allowing heat import has the most influence when the systems configuration has been limited to campus area. Limited space for electricity generation by renewable technologies causes that electrification of heat is possible to a lesser extent. In case (i) electricity production by WT for the operation of edHPs have been substituted by heat import and for case (ii) and (iii) and there is a direct substitution by heat import. With regard to Figure 5.6(i) and 5.7(d), at in between 50% and 60% CO_2 reduction the heat import for scenario 4B is substituted by additional boiler capacities, however the reason for this occurrence in the designs with higher emission reduction is yet unknown. The capacities of the installed storage options are substantially identical to the capacities of the storage options in scenario 3A and 3B. The storage distribution over the year is therefore for this scenario not discussed, since it is expected that this will not provide new insights.

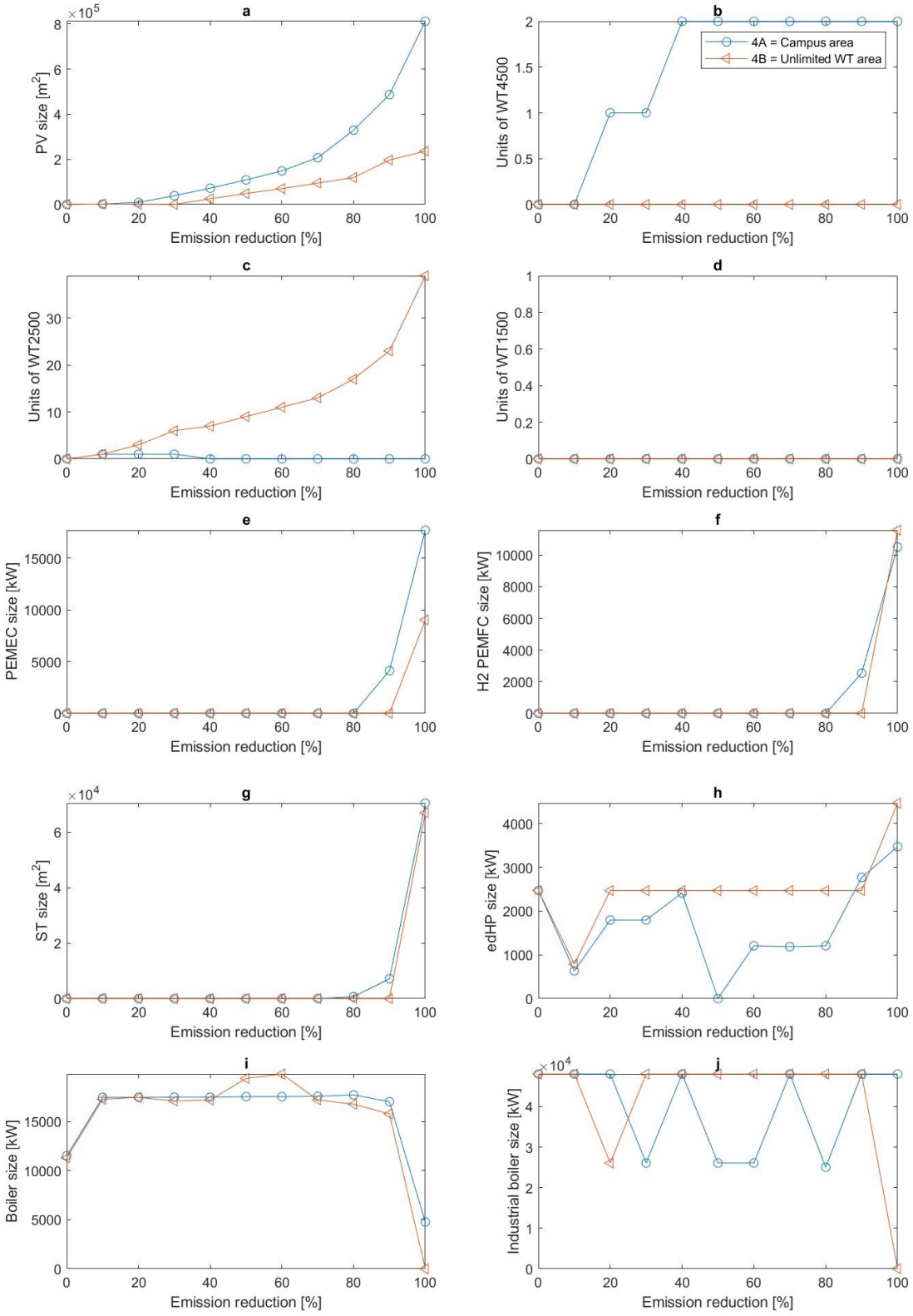

Figure 5.6: Size of the installed electricity and heat generating technologies along the Pareto fronts for scenario 4A (blue circle) and 4B (orange triangle) with (a) representing PV, (b) WT 4500, (c) WT 2500, (d) WT 1500, (e) PEMEC and (f) H2 PEMFC, (g) representing ST, (h) edHP, (i) boiler, (j) industrial boilers.

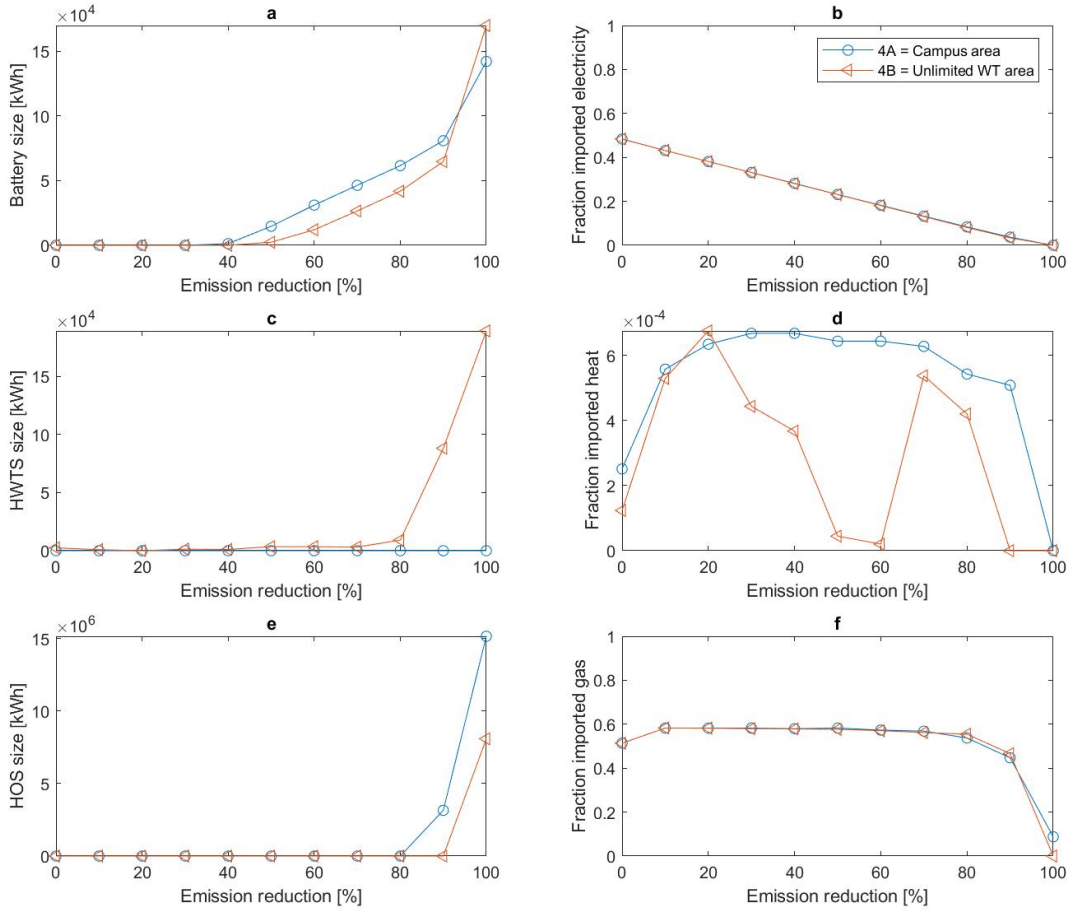

Figure 5.7: Size of the installed technologies storage technologies along the Pareto fronts for scenario 4A (blue circle) and 4B (orange triangle): (a) Battery, (c) HWTS and (e) HOS. Graph (b), (d), (f) represent the fraction imported electricity, heat and gas of the total energy used.

5.2.2 Geothermal heat versus green gas

Given the minor changes to the configuration of the optimal design with the current geothermal price, this section examines at what price it is more cost effective for UU to switch to geothermal heat supply by use of two scenarios; (i) reference and (ii) electrification of heat. The scenarios are carried out with a total cost objective, an MILP gap of 0.01 and with 365 typical days. Import of heat is not allowed.

Reference

The reference situation describes the price of operation of the current installations. Heat is provided by 48 MW of industrial boilers and 2.5 MW of existing edHPs. Accordingly, the set of technologies for the optimisation are existing edHPs and existing boilers. The considered of energy carriers are gas, heat and electricity, where import of gas and electricity is allowed. As result of the optimisation for the reference scenario, UU imports 9.8 GW h of green gas for heat provision by the industrial boilers and

11.9 GW h of electricity for heat production by the existing heat pumps, accounting for 0.72 mEUR yr^{-1} of operational costs, when the heat demand was equal to 50.6 GW h yr^{-1}. When determining the cost of heat in this scenario, the total annual costs are divided by the yearly heat demand. In the reference scenario the costs for heat amounts 0.0142 EUR kWh^{-1} heat demanded. The price for heat was lower than the price of the imported electricity and gas. This is caused by the presence of the heat pump, since this technology has a COP of approximately 3.5. The price for geothermal heat should in this case be below 3.90 EUR GJ^{-1}. However the Energy Team of UU mentioned to compensate with purchasing squared meters for greening. In 2018 UU compensated with 2.0 km^2, for which an amount of 0.11 EUR m^{-2} is charged. This means the costs increased with 0.22 mEUR yr^{-1}, resulting in a small cost increase for the reference case, of approximately 0.0044 EUR kWh^{-1}. Per 1.0 km^2 of greening, the geothermal heat price may increase with 0.0022 EUR kWh^{-1}.

Electrification of heat

This scenario determines at which price geothermal heat is competitive with a design that is based on electrification of heat. In this case edHP (new investments and existing), HWTS and electricity import are allowed. Accordingly, UU needed to invest in 4.4 MW of additional edHPs and 87.6 MW h of HWTS capacity. Accounting for an additional annual investment cost of 0.50 mEUR yr^{-1}, 0.008 mEUR yr^{-1} of maintenance cost and operational cost of 0.65 mEUR yr^{-1}, making a total annual costs of 1.17 mEUR yr^{-1}. Assuming the demand of the reference case, the cost for heat amounts 0.0231 EUR kWh^{-1} heat demanded, or 6.41 EUR GJ^{-1} .

5.2.3 Emission free geothermal heat

This section examines scenario 4C and 4D of Section 3.5. In the previous optimisations, emissions are allocated to the use of geothermal energy. However, this scenario assumes that the electricity used for geothermal energy is 100% sustainable. Accordingly, the threshold at which a switch should be made from local generation to geothermal heat import can be determined. Figure 5.8 shows the Pareto fronts for scenario 4C and 4D (Section 3.5) when geothermal heat import is 100 % renewable. As expected, full decarbonisation could as well in scenario 4C as in 4D be achieved. In scenario 4C, the annual costs for energy import of decreases till 80%, while beyond 80% the annual costs for energy import increases. For scenario 4D, geothermal heat import is available at low cost and accompanied with zero emissions. In this scenario the costs for import already increase from 70 %. Table 5.3 shows the relative cost increase. it worth noticing that the substantial cost reduction of emission free geothermal heat only slightly influences the cost of the designs.

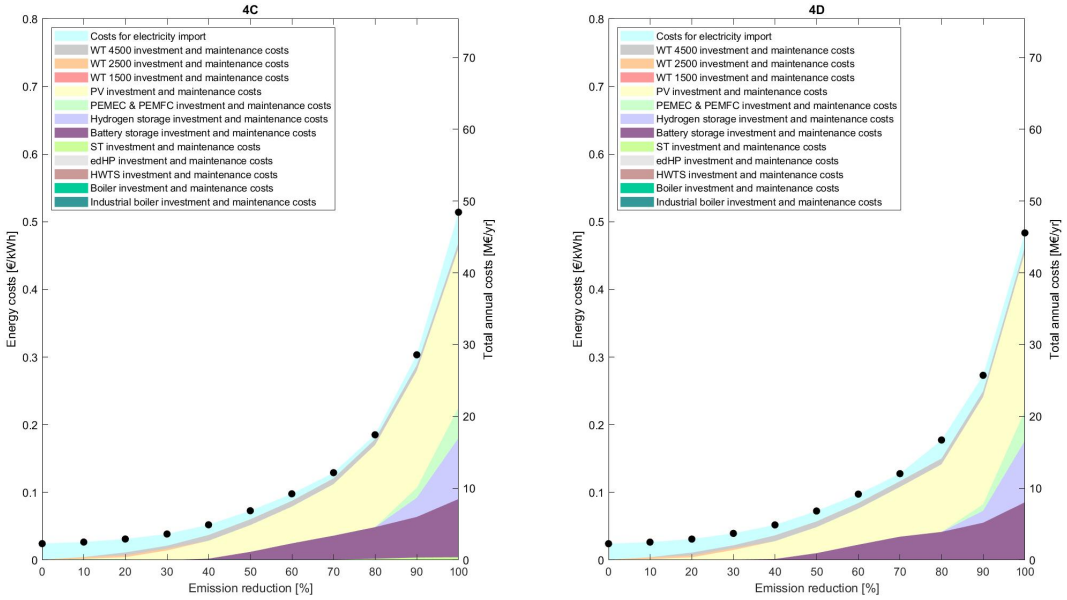

Figure 5.8: Cost-emission Pareto front for sub-scenario 4 for electricity and heat supply to UU with as available set of technologies; WTs, PV panels, LiB, PtG, edHP, boilers, industrial boilers, ST and HWTS for scenario (4C) the campus property and scenario (4D) also at campus property by import geothermal heat available at low costs. In this scenario import of electricity, geothermal heat and gas is allowed. Geothermal heat import is in this case accompanied with zero emissions.

Table 5.3: Relative cost increase per emission reduction achieved by the design compared to reference for scenario (4C) campus area with zero emission geothermal heat import and (4D) at campus area with zero emission geothermal heat import at low costs (6 EUR/GJ). The bold value indicates the maximum emission reduction that can be achieved if electricity costs are not more than doubled.

CO_2 emission reduction	Relative cost increase (4C) [%]	Relative cost increase (4D) [%]
Reference	-	-
10 %	9.5 %	9.4 %
20 %	28.1 %	28.2 %
30 %	**58.7 %**	**62.9 %**
40 %	114.7 %	114.9 %
50 %	200.4 %	199.7 %
60 %	303.5 %	302.9 %
70 %	432.1 %	428.1 %
80 %	662.9 %	633.7 %
90 %	1150.1 %	1029.0 %
100 %	2018.5 %	1899.4 %

From Figure 5.9(b)(c), it can be observed that for scenario 4C, gas is substituted by geothermal heat from upwards 80 % emission reduction, while for scenario 4D is occurs already at 50 %. Although Pareto fronts 4C and 4D (Figure 5.8) show little differences, the price drop of geothermal heat certainly influenced the substitution of gas in the designs.

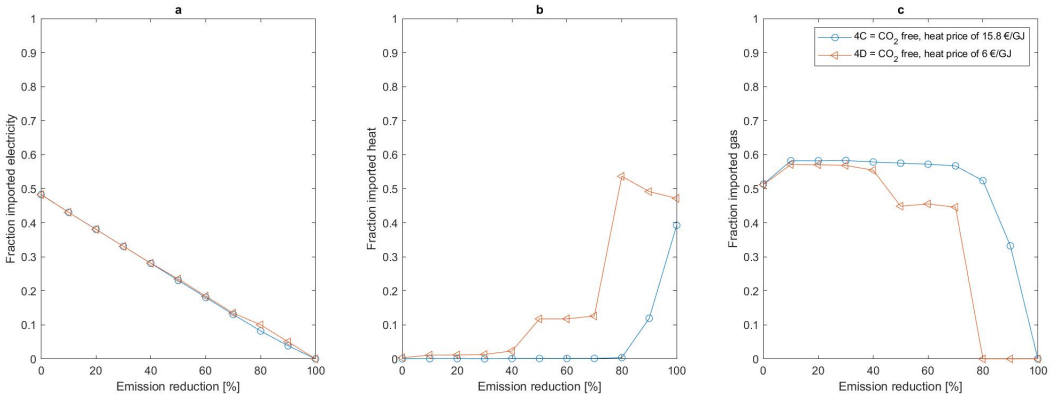

Figure 5.9: Fraction of imported energy of total energy demand for scenario 4C and 4D, with (a) electricity, (b) geothermal heat and (c) gas.

Chapter 6

Sensitivity of system costs

To determine the certainty of the proposed energy system designs, a sensitivity analysis is performed on the available (i) area for PV and ST (ii) for the energy prices of gas and electricity and for (iii) for the heat demand, given that the analysed area for renewable energy technologies might be partly redefined, energy prices probably rise from now till 2030 and the assumed energy demand for 2030 is based on expectations. The sensitivity of the system costs are only tested for scenario 3A, which Pareto front is seen as the reference.

6.1 Solar area

The energy team expressed an interest to explore two scenarios for the solar area; 20 000 m^2 and 75 000 m^2 available land for ST and PV. Therefore these values are used for the sensitivity, of which the Pareto fronts are shown in Figure 6.1. The sensitivity analysis performed shows the maximum achievable emission reduction of 27 % and 45 % for 20 000 m^2 and 75 000 m^2 of available land respectively. The amount of area available certainly has effect on the feasibility of a total decarbonised system.

6.2 Energy prices

Energy prices vary and are hard to predict. Therefore, the sensitivity of system costs are analysed for electricity and gas. However, no sensitivity analysis is performed for the price of geothermal heat import this has already been examined by scenario 4D (Section 5.2.3). The sensitivity of the system for varying energy prices is analysed by increasing the import price of electricity by 25% and by 50%, since energy prices are expected to rise in the future. Gas prices are expected to increase by 75 % in 2030, therefore this sensitivity analysis is performed with an 50 % and 100 % price increase. Figures 6.2 and 6.3 show the sensitivity of the systems costs for electricity and gas respectively. Figure 6.2 indicates that electricity price increase only effects the systems cost at designs with low emissions reductions. The reason for this occurrence is rather straightforward, since the share of electricity import is higher in these designs. However, looking at Figure 6.3, increase in gas prices have little to no effect on systems costs.

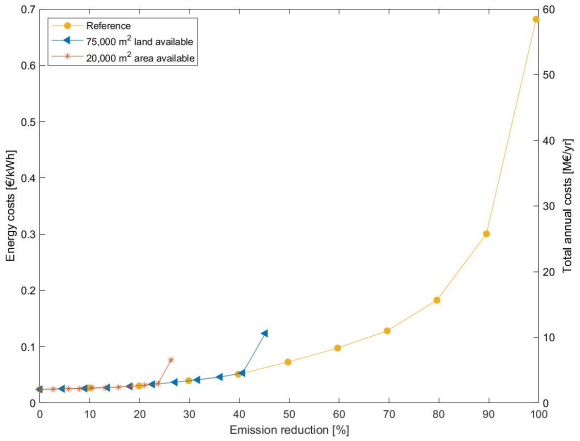

Figure 6.1: Cost emission Pareto front for three scenarios assessing different areas available for PV and ST installation, namely: (i) Reference 1 289 014 m^2 (ii) 75 000 m^2 and (iii) 20 000 m^2 to determine the sensitivity of the systems costs for scenario 3A (Section 3.5).

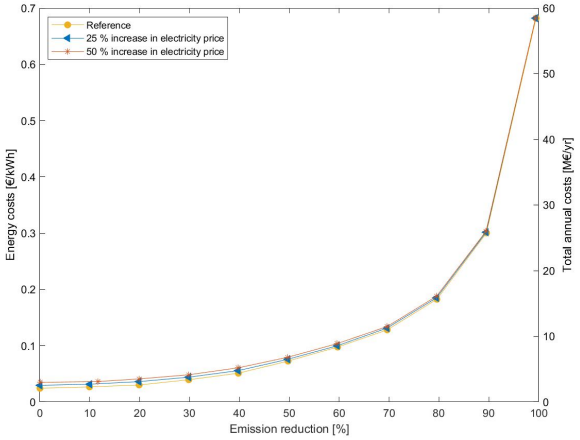

Figure 6.2: Cost emission Pareto front for three scenarios assessing different prices for electricity import, namely: (i) Reference (ii) 25 % increase in price and (iii) 50 % increase in price to determine the sensitivity of the systems costs for scenario 3A (Section 3.5).

6.3 Energy demand

Another uncertainty is the expected demand in 2030. However, based on the real estate developments, the heat demand will decrease by 60 percent from now towards 2030, whereas electricity demand was predicted to remain the same [3]. The analyses excluded approximately 30% of the buildings in the calculation of the thermal demand. Therefore, the sensitivity of analysis is performed with an 30% thermal demand increase and from this point a 60% heat demand decrease. Resulting in a difference of 43 % demand increase compared to reference and 43 % decrease.

As expected, the system costs rise upon an increase in demand an decreased for decreased demands (Figure 6.4). The maximum achieved decarbonisation is also effected by the thermal demand in or decrease. In case thermal demand is increased, the maximum emission reduction that can be achieved

is 99.17 %, while in case of decrease the maximum is 99.61 %. However, in all three cases full decarbonisation is unfeasible at the campus.

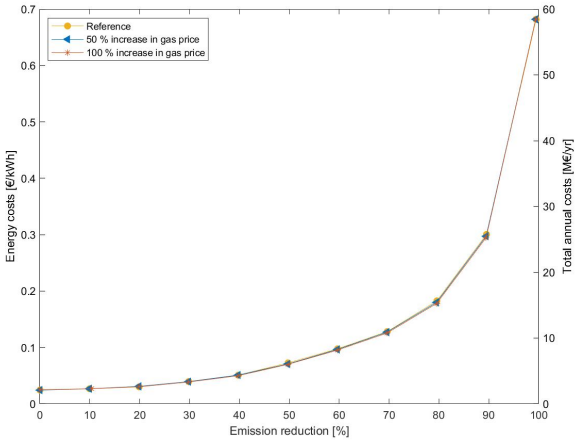

Figure 6.3: Cost emission Pareto front for three scenarios assessing different prices for electricity import, namely: (i) Reference (ii) 50 % increase in price and (iii) 100 % increase in price to determine the sensitivity of the systems costs for scenario 3A (Section 3.5).

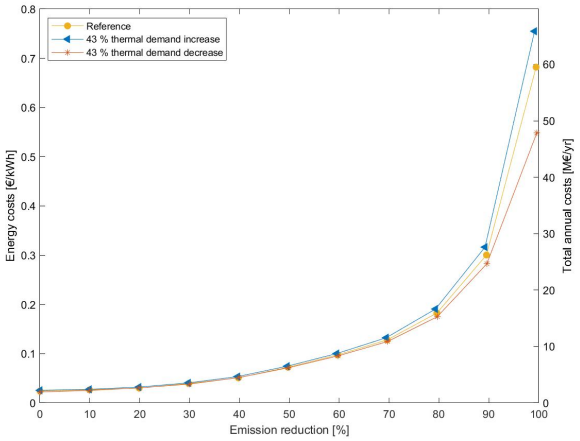

Figure 6.4: Cost emission Pareto front for three scenarios assessing different thermal demand, namely: (i) Reference (ii) 43 % decrease in thermal demand and (iii) 43 % decrease in thermal demand to determine the sensitivity of the systems costs for scenario 3A (Section 3.5).

Chapter 7

Discussion

Some insightful results have been obtained from the configurations discussed in Chapter 4 and 5. Both scenarios show that compensation of the seasonal mismatch is important in designs with higher emission reductions, while day to day storage (e.g. LiB and HWTS) are at emission reduction higher than 40%. Up to now, UU mainly focused on the implementation of PV, while wind turbines are actually more cost effective based on the results of the optimisations. In addition, installing wind turbines also has a positive effect on the need for seasonal storage. Designs with a large share of WTs need seasonal storage for CO_2 reductions higher than 90%, while the threshold lowers to 80% for small amount of installed WTs. In addition, the unlimited area for wind turbines ensures lower system costs. However, for 100% reduction 39 wind turbines are installed. Accordingly, UU would need approximately 20 km^2 of additional land, which can not be achieved next to the campus. Nevertheless, electricity losses through grid are almost negligible, so an area elsewhere could also be used for installation of wind turbines for UU.

In general, there was a clear preference for PV installation rather than ST. This is probably caused by the fact that the E-Hub tool only contains a seasonal electricity storage. Overproduction of PV in summers can be used for electricity and heat supply in winters using the PtG technology, which is not the case for ST. In addition, all examined scenarios show that LiB is required for designs with higher emission reductions than 40 %. Furthermore, full decarbonisation at campus area can not be achieved with local energy generation. The maximum decarbonisation that could be achieved in scenario 3A and 4A is respectively, 99.48 and 99.39. Last, ST is only installed in designs with emission reductions higher than 80 %, which causes that HWTS is also used above this Pareto front point.

An important first step in decarbonising the energy supply is to have a good overview of the energy consumed. Outdated measuring systems caused that a number of assumption had to be made regarding the energy demand of UU. Although conservative assumptions are made, the used data may deviate from reality. With regard to the input data used, emission factors are assigned to green energy during this study, motivated by the fact that the purchase of 'green' energy may not encourage local generation of renewable energy [51] and to give a better presentation of the reality. People with a different perspective can possibly criticise this assumption. However, the GO trading mechanism ensures that RETs are installed where it is most cost effective, this adversely affects the share of RETs in the Netherlands, since the total share of contractual sold green electricity was 64 % in 2015, while

the total generated green electricity amounted to 12 % [52][47]. Nonetheless, this study focuses on CO_2 reduction at micro level at which UU should be a role model in sustainable energy generation, making this perspective correspond with the chosen assumption. On the contrary, the results are presented in levels of decarbonisation. If the ratios between the emissions related to the different imported energy carriers are kept equal, increase or decrease of the emission factors should not affect the configurations. In the first place, the cost data used for the selected technologies may affect the optimal designs, since they are only partially adjusted to current investment costs. Especially PtG is a fairly new technology and presence of this technology in the designs causes that systems costs rise considerably. However, costs for PtG will probably decrease over the years as the technology is more proven and in use. Additionally, UU prefers the use of ATES systems in combination with edHPs. Integration of the ATES technology in the optimisation would allow to check whether this configuration is the most cost effective. Unfortunately, the E-Hub does not contain the ATES technology in its current state. Also, standing charge and taxes are not included in the energy import, which probably financially disadvantaged the renewable energy technologies. Furthermore, it was also impossible to exclude double counting as edHPs are used, for which electricity demand and heat demand is registered in the data bases of UU. However, by performing a sensitivity analysis, an attempt has been made to get a grip on this. Lastly, the optimisations in Chapter 4 and 5 are performed with one node. As a result, flows could not be optimised, losses through networks were not included, and neither were construction costs for connecting a number of buildings to the existing network. However, the heat network is distributed from Northwest to Southeast of campus, so only short distance pipelines have to be installed. Furthermore, a pipe for geothermal heat import is not considered. Construction costs for the pipe are assumed to be captured within the cost decrease of geothermal heat import over the years.

Recommendations Based on the research process and the optimal designs obtained, a number of recommendations are proposed. First recommendations for UU are considered, followed by recommendations for the E-Hub model.

Considering the missing data and incorrect registrations of the current measuring systems, UU should certainly invest in smart metering systems. The energy consumed by UU should be transparent at any moment in time. Additionally, UU should invest in renewable electricity production at the campus site rather than heat production. Area available at the campus must be used optimally for wind turbines and on a smaller scale PV. In addition, PtG is a promising seasonal storage technology, but to date the costs of this are still too high in the proposed designs. It is also only necessary to add this seasonal storage to the system if 80% is generated locally. By that time, PtG is probably more affordable. If 100% emission free geothermal heat can be provided from the by the geothermal plant at a price of $15.8\,\mathrm{EUR\,GJ^{-1}}$, substituting gas by geothermal heat is favourable for emission reductions higher than 80%. However, if the price drops to $6\,\mathrm{EUR\,GJ}$, the gas import should be substituted by geothermal heat at 50% emission reduction. Nevertheless, when geothermal heat is not fully decarbonised, it will only partly substitute the HWTS.

The E-Hub should be expanded with ATES. The ATES technology is currently well known and a promising option for future heat supply in combination with edHP. When ATES is added to the set of

technologies, the optimal ratios between installed capacity of ATES and edHP could be determined. Moreover, the prices of the E-Hub should be updated, but it would also be useful if the tool could take into account the price decrease of investment in RES (e.g. by the learning curve in case of new technologies) when a prediction is made of an optimal energy system for the future.

Chapter 8

Conclusion

This research aims to analyse to what extend UU could have the energy demand covered by local generation at the campus to determine the effects of the limited area and to indicate the quick wins in CO_2 reduction as well as the maximum achievable reduction. By performing a multi objective optimisation for cost and emissions, the Pareto optimal designs of the energy system are identified. The presented research is carried out by applying the E-Hub, an in-house, MILP-based energy system modelling tool, which was originally developed by Gabrielli et al. (2018) [11] Gabrielli et al. (2018a) [10]. Application of this tool allowed to identify whether a fully decarbonised local energy system could be achieved based on the input data for UU. Two scenarios are analysed; (I) where UU only wants to decarbonise its electricity supply and (II) where UU wants to decarbonise their whole energy supply (e.g. electricity and heat supply). The two scenarios are both divided into two sub-scenarios, which are subsequently divided into particular cases. For a detailed overview of the analyses performed, see Figure 3.9 Section 3.5.

According the results of Chapter 4, full decarbonisation of electricity supply can be achieved with local generation at the campus. Sub-scenario 1 and 2 have demonstrated that there is indeed a need for seasonal storage in the designs with higher emission reductions. This makes sub-scenario 2, with PTG the cheaper option to achieve full decarbonisation. However, the related costs for electricity supply with use of PtG are approximately $43\,\mathrm{mEUR\,yr^{-1}}$ in case the energy system is completely located at the campus (scenario 2A) and $31\,\mathrm{mEUR\,yr^{-1}}$ if wind turbines could be installed outside the campus (scenario 2B). Financially speaking, both configurations are unfeasible for UU, since the electricity cost would rise to $0.97\,\mathrm{EUR\,kWh^{-1}}$ for case 2A and $0.71\,\mathrm{EUR\,kWh^{-1}}$ for case 2B. Compared to the reference, the costs for full decarbonisation are extremely high, since electricity costs are increased by a factor of approximately 21 and 15, for scenario 2A and 2B respectively. Speaking of the most carbon-cost effective options for case 2A and 2B, 30 % and 40% CO_2 reduction can be achieved. In this case carbon-cost effective referred to a maximum threshold of 2 times the reference electricity price. The optimal design at 30% emission reduction of scenario 2A contains 2 WTs of 4500 kW and $38\,969\,\mathrm{m^2}$ of PV panels.

With regard to the second scenario, Chapter 5 demonstrated that it is impossible to reach full decarbonisation when the entire energy provision is generated and stored at the campus. The maximum of CO_2 reduction achieved in scenario 3A and 4A are 99.48% and 99.39% respectively. When

the area is not limited for installation of WTs, which is in case 3B and 4B, full decarbonisation could be achieved. However, the costs for complete decarbonisation for these sub-scenarios are also economically infeasible. Important is that the designs show that investment should be focused on electricity generation rather than heat production. With regard to the most carbon-cost effective option for the limited area of the campus (scenarios 3A and 4A), the maximum CO_2 reduction that can be achieved is 30%, while in scenarios 3B and 4B an additional 10% reduction could be obtained with $3.6\,\mathrm{km}^2$ of additional land for installation of 5 extra WTs of 2500 kW. The average energy price of 3A and 4A at 30 % reduction is around $0.040\,\mathrm{EUR\,kWh}^{-1}$ in both cases. In general, the designs along the Pareto points are barely influenced by the allow of geothermal heat import. Considering that it is yet uncertain whether geothermal heat becomes available, the configuration of the design at this point is only discussed for case 3A. The optimised system contains $39\,386\,\mathrm{m}^2$ of PV, 1 WT of 4500 kW and 1 of 2500 kW and an additional boiler capacity of approximately 18 MW, existing industrial boilers are fully utilised and edHPs are used at half capacity. If geothermal heat can be supplied with zero emission, the threshold for UU to switch from gas to geothermal heat is at more than 80% emission reduction if geothermal heat is offered at $15.8\,\mathrm{EUR\,GJ}^{-1}$ and 50 % when it is supplied at a price of $6\,\mathrm{EUR\,GJ}^{-1}$. Contribution to the geothermal project is based on expectations not yet profitable for UU. Extending edHP and HWTS capacity is more cost effective for the given assumptions, since geothermal heat price should drop below $6.41\,\mathrm{EUR\,GJ}^{-1}$ to be competitive with this design.

Bibliography

[1] European Union. Energy roadmap 2050 Energy. *Publications Office of the European Union*, pages 1–20, 2012.

[2] P. Mancarella. Multi-energy systems: An overview of concepts and evaluation models. *Energy*, 65:1–17, 2014.

[3] Province of Utrecht. A climate for energy transition [Een klimaat voor energietransitie]. Technical report, 2016.

[4] M. Weustink-van Ditzhuyzen, F. Sybesma, Direction Real Estate & Campus, and Utrecht University. Ambition document Utrecht Science Park [Ambitiedocument Utrecht Science Park]. Technical report, 2018.

[5] University Utrecht. Universiteit Utrecht helpt gemeenten om woningen van het gas af te krijgen. https://www.uu.nl/nieuws/universiteit-utrecht-helpt-gemeenten-om-woningen-van-het-gas-af-te-krijgen, 2018. [Online; accessed 04/10/2019].

[6] Utrecht University. De aarde als energiebron. https://www.uu.nl/nieuws/de-aarde-als-energiebron, 2018. [Online; accessed 04/10/2019].

[7] H. Ren and W. Gao. A MILP model for integrated plan and evaluation of distributed energy systems. *Applied Energy*, 87(3):1001–1014, 2010.

[8] M. Schulze, L. Friedrich, and M. Gautschi. Modeling and optimization of renewables: Applying the energy hub approach. *IEEE International Conference on Sustainable Energy Technologies*, (December 2008):83–88, 2008.

[9] S. Weitemeyer, D. Kleinhans, T. Vogt, and C. Agert. Integration of Renewable Energy Sources in future power systems: The role of storage. *Renewable Energy*, 75:14–20, 2015.

[10] P. Gabrielli, M. Gazzani, and M. Mazzotti. Electrochemical conversion technologies for optimal design of decentralized multi-energy systems: Modeling framework and technology assessment. *Applied Energy*, 221:557–575, 2018.

[11] P. Gabrielli, M. Gazzani, E. Martelli, and M. Mazzotti. Optimal design of multi-energy systems with seasonal storage. *Applied Energy*, 219:408–424, 2018.

[12] E. Pfeiffer. Scenarios Energy Vision Energy Neutral Utrecht East 2030 [Scenario's Energievisie Energieneutraal Utrecht Oost 2030]. Technical report, 2017.

[13] M. Geidl. Integrated Modeling and Optimization of Multi-Carrier Energy Systems. 2007.

[14] M. Geidl. Energy Hubs for the Future. *IEEE Power and Energy Magazine*, 5:pp. 24–30, 2007.

[15] K. Hemmes, J. L. Zachariah-Wolf, M. Geidl, and G. Andersson. Towards multi-source multi-product energy systems. *International Journal of Hydrogen Energy*, 32(10-11):1332–1338, 2007.

[16] E. Fabrizio, V. Corrado, and M. Filippi. A model to design and optimize multi-energy systems in buildings at the design concept stage. *Renewable Energy*, 35(3):644–655, 2010.

[17] Y. Wang, N. Zhang, C. Kang, D. S. Kirschen, J. Yang, and Q. Xia. Standardized Matrix Modeling of Multiple Energy Systems. *IEEE Transactions on Smart Grid*, 10:257–270, 2019.

[18] O. Ellabban, H. Abu-Rub, and F. Blaabjerg. Renewable energy resources: Current status, future prospects and their enabling technology. *Renewable and Sustainable Energy Reviews*, 39:748–764, 2014.

[19] R. Kumar and M.A. Rosen. A critical review of photovoltaic-thermal solar collectors for air heating. *Applied Energy*, 88(11):3603–3614, 2011.

[20] C. Winterscheid. Integration of solar thermal systems in existing district heating systems. *Euro-heat and Power (English Edition)*, 14(4):16–20, 2017.

[21] F. A. Peuser, K. H. Remmers, and M. Schnauss. *Solar Thermal Systems - Succesful Planning and Construction*, volume 53. 2010.

[22] N. P. Garcia, K. Vatopoulos, A. K. Riekkola, A. Perez Lopez, and L. Olsen. Best available technologies for the heat and cooling market in the European Union. *JRC Scientific and policy reports*, 2012.

[23] T. J. Chang, Y. T. Wu, H. Y. Hsu, C. M. Liao, and C. R. Chu. Assessment of wind characteristics and wind turbine characteristics in Taiwan. *Renewable Energy*, 28(6):851–871, 2003.

[24] J. Brenn, P. Soltic, and C. Bach. Comparison of natural gas driven heat pumps and electrically driven heat pumps with conventional systems for building heating purposes. *Energy and Buildings*, 42(6):904–908, 2010.

[25] L. Lu, X. Han, J. Li, J. Hua, and M. Ouyang. A review on the key issues for lithium-ion battery management in electric vehicles. *Journal of Power Sources*, 226:272–288, 2013.

[26] B. Diouf and R. Pode. Potential of lithium-ion batteries in renewable energy. *Renewable Energy*, 76:375–380, 2015.

[27] A. Jossen, J. Garche, and D. U. Sauer. Operation conditions of batteries in PV applications. *Solar Energy*, 76(6):759–769, 2004.

[28] S. B. Walker, U. Mukherjee, M. Fowler, and A. Elkamel. Benchmarking and selection of Power-to-Gas utilizing electrolytic hydrogen as an energy storage alternative. *International Journal of Hydrogen Energy*, 41(19):7717–7731, 2016.

[29] L.F. Cabeza. *Advances in Thermal Energy Storage Systems: Methods and Applications*. 2014.

[30] M. Bloemendal and N. Hartog. Analysis of the impact of storage conditions on the thermal recovery efficiency of low-temperature ATES systems. *Geothermics*, 71:306–319, 2018.

[31] Rijksinstituut voor Volksgezondheid en Milieu (RIVM). Een literatuurstudie naar de mogelijke risico's van warmte- en koudeopslag voor de grondwaterkwaliteit. Technical Report RIVM Rapport 607050009/2011, 2011.

[32] D. Vermaas and L. van Wee. Warmte-koudeopslag in de bodem kan efficienter. 2009.

[33] Gurobi. Mixed-Integer Programming (MIP) - A Primer on the Basics Branch-and-Bound. http://www.gurobi.com/resources/getting-started/mip-basics, 2018. [Online accessed 19/09/2019.

[34] R. Yokoyama, Y. Shinano, S. Taniguchi, M. Ohkura, and T. Wakui. Optimization of energy supply systems by MILP branch and bound method in consideration of hierarchical relationship between design and operation. *Energy Conversion and Management*, 92:92–104, 2015.

[35] J. Löfberg. Yalmip : A toolbox for modeling and optimization in matlab. In *In Proceedings of the CACSD Conference*, Taipei, Taiwan, 2004.

[36] E. Klotz and A. M. Newman. Practical guidelines for solving difficult mixed integer linear programs, 2013.

[37] P. Gabrielli, . Fürer, G. Mavromatidis, and M. Mazzotti. Robust and optimal design of multi-energy systems with seasonal storage through uncertainty analysis. *Applied Energy*, pages 1192–1210, 2019.

[38] KNMI. Uurgegevens van het weer in nederland. https://projects.knmi.nl/klimatologie/uurgegevens/selectie.cgi. [Online; accessed 22/02/2019].

[39] W. van Sark, A. de Waal, J. Uithol, N. Dols, F. Houben, R. Kuepers, M. Scherrenburg, B. van Lith, and F. Benjamin. Energy performance of a 1.2 MWp photovoltaic system distributed over eight buildings at Utrecht University Campus. In *33rd European Photovoltaic Solar Energy Conference and Exhibition*, pages 2284–2287, 2017.

[40] D. Huitink, S. Raaijmakers, L.E. Schreurs, and B. Vonsée. Plaatsmaken voor PV. 2018.

[41] D. Huitink, S. Raaijmakers, L.E. Schreurs, and B. Vonsée. Een zonnige toekomst. 2018.

[42] L. Cornax. Duurzame energie uit wind op de Uithof Inventarisatie van mogelijkheden Inventarisatie van mogelijkheden. 2018.

[43] DaftLogic. Google Maps Area Calculator Tool. https://www.daftlogic.com/projects-google-maps-area-calculator-tool.htm, 2015. [Online; accessed 04/04/2019].

[44] Innax. Eview 4.0. https://www.eview.nl/#/login. [Online; accessed 08/05/2019].

[45] van Beek Ingenieurs. Erbis energiemonitoring. http://www.erbisonline.nl/. [Online; accessed 08/05/2019].

[46] Minder gas. Degree day calculator. https://www.mindergas.nl/degree_days_calculation. [Online; accessed 14/08/2019].

[47] CBS. Elektriciteit en warmte - productie en inzet naar energiedrager. https://opendata.cbs.nl/statline/#/CBS/nl/dataset/80030ned/table?ts=1559831857118. [Online; accessed 05/06/2019].

[48] RVO. Berekening van de standaard CO2-emissiefactor aardgas. Technical report, 2017.

[49] N. Hoogervorst. Toekomstbeeld Klimaatneutrale Warmtenetten in Nederland. *Uitgeverij PBL*, page 80, 2017.

[50] P. Lako, S.L. Luxembourg, A.J. Ruiter, and B. in 't Groen. Geothermische energie en de SDE. Technical report, 2011.

[51] D. Toke. Renewable financial support systems and cost-effectiveness. *Journal of Cleaner Production*, 15(3):280–287, 2007.

[52] J.A.M. Hufen. Cheat electricity? The political economy of green electricity delivery on the dutch market for households and small business. *Sustainability (Switzerland)*, 9(1), 2017.

Appendix A

Utrecht University Campus

A.1 Campus map

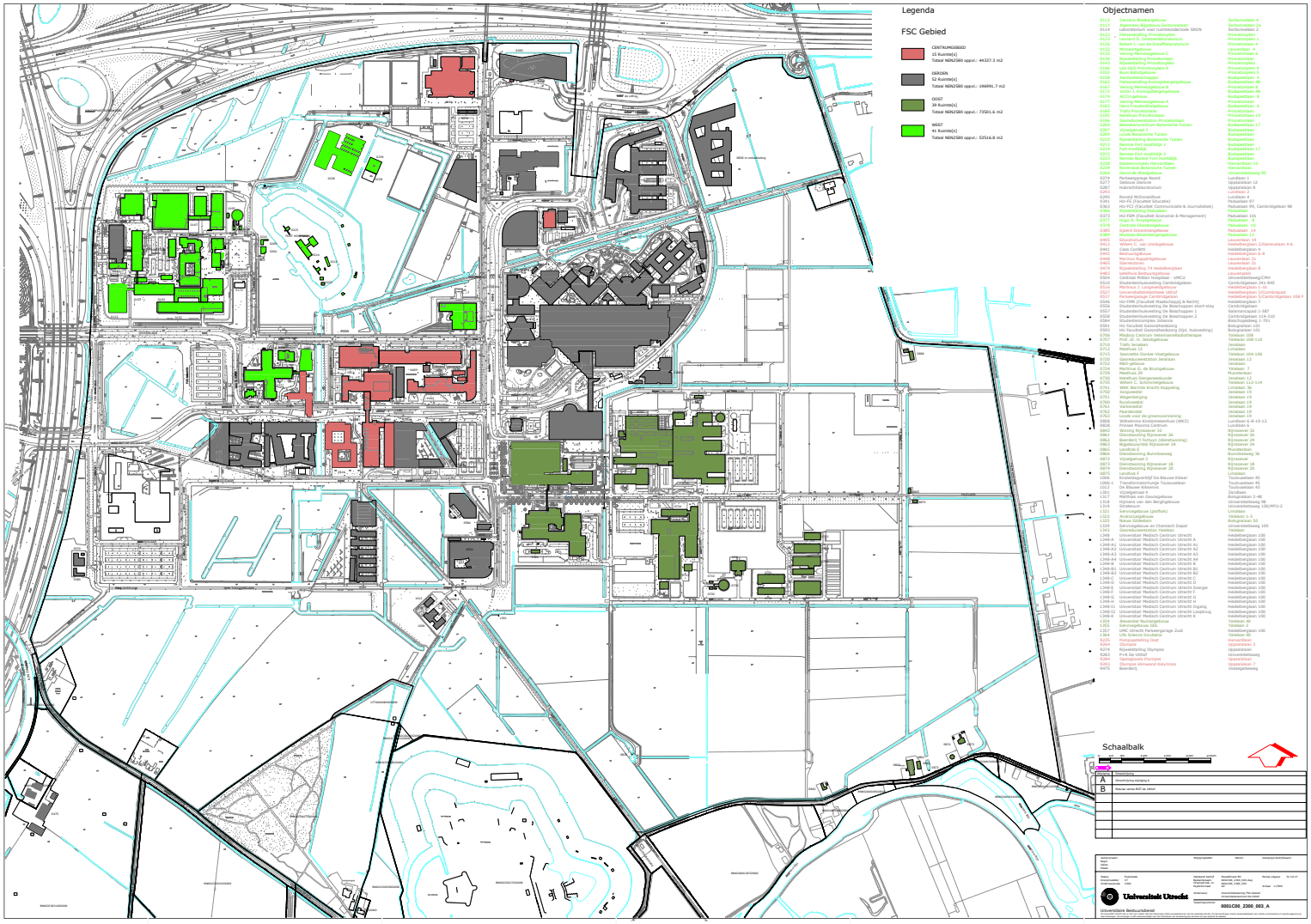

Figure A.1: Map of USP, where the buildings in green, red and dark green are the buildings owned by UU.

A.2 Energy use Utrecht University 2018

Table A.1: Expected annual electricity and heat demand of UU of year 2018 listed per building and the total annual energy supply by the existing PV panels and ATES system of UU. The total electricity demand of UU is determined by the sum of the demand of the buildings minus the PV generation. The total annual heat demand is the sum of the heat demand per building minus the ATES systems heat generation. The optimisations are performed based on this annual energy demand of UU.

Building	Electricity	Heat
01.12 Bleekergeb. (Sorbonnelaan 4)	462 116 kW h	504 722 kW h
01.23 Ornsteinlab. (Princetonplein 1)	1 023 146 kW h	1 431 111 kW h
01.26 ESL/v.d. Graaff. (Princetonlaan 4)	165 070 kW h	N/A
01.32 Minnaertgebouw (Leuvenlaan 4)	562 037 kW h	N/A
01.35 NITG-TNO (Princetonlaan 6)	840 965 kW h	1 501 111 kW h
01.52 Buys Ballot lab. (Princetonpl. 5)	1 855 737 kW h	2 705 278 kW h
01.58 Aardwetenschappen (Budapestlaan 4)	775 808 kW h	966 389 kW h
01.67 V. Meinesz B (Princetonlaan 8)	624 730 kW h	N/A
01.72 OWC: V.13 Koningsberger (Budap.ln2)	1 870 945 kW h	144 167 kW h
01.74 ACCU (Budapestlaan 8)	403 940 kW h	527 500 kW h
01.77 Vening Meineszgebouw A (GEO)	893 113 kW h	N/A
01.83 Wiskunde gebouw (Budapestlaan 6)	167 489 kW h	N/A
02.14 Fort Hoofddijk (Budapestlaan 17)	126 488 kW h	38 890 kW h
02.28 Res.kas+Bot.tuin (Uppsalaln Tuin)	432 209 kW h	2 190 278 kW h
02.60 D.de Wiedgeb (Universiteitswg 99)	4 061 913 kW h	4 171 944 kW h
03.77 Hugo Kruytgebouw (Padualaan 8)	5 463 135 kW h	9 121 111 kW h
03.85 S Groenmangeb CGN (Padualn 14)	40 791 kW h	535 556 kW h
03.89 Bloembergen geb./NMR(Padualaan 12)	725 223 kW h	N/A
04.05 Educatorium (Leuvenlaan 19)	1 027 076 kW h	1 255 556 kW h
04.12 vUnnikgeb /Tr 2 (Heidelbergln 2)	1 057 374 kW h	1 352 500 kW h
04.42 Bestuursgebouw (Heidelberglaan 8)	818 323 kW h	1 206 389 kW h
04.48 M.Ruppertgeb./Tr.1(Leuvenlaan 21)	387 902 kW h	854 444 kW h
05.16 Langeveld geb (Heidelberglaan 1)	1 029 003 kW h	N/A
05.27 Univers.Bibliot (Heidelberglaan 3)	3 052 791 kW h	2 148 056 kW h
07.07 Klin. Gez.dieren/Jakob (Yaleln 8)	1 670 051 kW h	3 594 032 kW h
07.15 JDonker-Voet geb(Yaleln 104-106)	1 572 788 kW h	N/A
07.24 Landb.dieren/de Bruin (Yaleln.7)	1 276 733 kW h	N/A
07.35 Klin. Heelk./Schimmel (Yaleln 112)	2 100 045 kW h	2 640 245 kW h
07.50 Jongveestal(Tolakker)	381 579 kW h	N/A
13.22 Androclusgebouw (Yaleln 1)	3 783 523 kW h	10 030 000 kW h
13.25 Nw Gildestein (Yaleln 2)	3 615 954 kW h	N/A
13.54 Alexander Numan geb.(Yaleln.40-60)	1 595 008 kW h	645 024 kW h
13.64 LSI (Yalelaan 62)	N/A	552 222 kW h
92.64 Olympos	881 128 kW h	729 444 kW h
Total use Utrecht University	44 744 123 kW h	48 845 968 kW h
PV generation	1 075 128 kW h	
ATES generation		1 722 015 kW h
Total demand Utrecht University	43 668 995 kW h	47 123 953 kW h

A.3 Energy networks Campus

Table A.2: The existing connections to UU heat network and ATES system listed per building. Yes indicates the building is connected, while no means there is no connection.

Building	UU heat network connection	ATES system connection
01.12 Bleekergeb. (Sorbonnelaan 4)	Yes	No
01.23 Ornsteinlab. (Princetonplein 1)	Yes	Yes
01.26 ESL/v.d. Graaff. (Princetonlaan 4)	Yes	Yes
01.32 Minnaertgebouw (Leuvenlaan 4)	Yes	Yes
01.35 NITG-TNO (Princetonlaan 6)	Yes	Yes
01.52 Buys Ballot lab. (Princetonpl. 5)	Yes	No
01.58 Aardwetenschappen (Budapestlaan 4)	Yes	No
01.67 V. Meinesz B (Princetonlaan 8)	Yes	Yes
01.72 OWC: V.Koningsberger (Budap.ln2)	Yes	Yes
01.74 ACCU (Budapestlaan 8)	Yes	No
01.77 Vening Meineszgebouw A (GEO)	Yes	Yes
01.83 Wiskunde gebouw (Budapestlaan 6)	No	No
02.14 Fort Hoofddijk (Budapestlaan 17)	Yes	No
02.28 Res.kas+Bot.tuin (Uppsalaln Tuin)	Yes	No
02.60 D.de Wiedgeb (Universiteitswg 99)	Yes	No
03.77 Hugo Kruytgebouw (Padualaan 8)	Yes	No
03.85 S Groenmangeb CGN (Padualn 14)	No	No
03.89 Bloembergen geb.(Padualaan 12)	No	No
04.05 Educatorium (Leuvenlaan 19)	No	No
04.12 vUnnikgeb /Tr 2 (Heidelbergln 2)	No	No
04.42 Bestuursgebouw (Heidelberglaan 8)	No	No
04.48 M.Ruppertgeb./Tr.1(Leuvenlaan 21)	No	No
05.16 Langeveld geb (Heidelberglaan 1)	No	No
05.27 Univers.Bibliot (Heidelberglaan 3)	Yes	No
07.07 Klin. Gez.dieren/Jakob (Yaleln 8)	Yes	No
07.15 JDonker-Voet geb(Yaleln 104-106)	Yes	No
07.24 Landb.dieren/de Bruin (Yaleln.7)	Yes	No
07.35 Klin. Heelk./Schimmel (Yaleln 112)	Yes	No
07.50 Jongveestal(Tolakker)	No	No
13.22 Androclusgebouw (Yaleln 1)	Yes	No
13.25 Nw Gildestein (Yaleln 2)	Yes	No
13.54 Alexander Numan geb.(Yaleln.40-60)	Yes	No
13.64 LSI (Yalelaan 62)	No	No
92.64 Olympos (Uppsalalaan 3)	No	No

A.3.1 Heat network connections

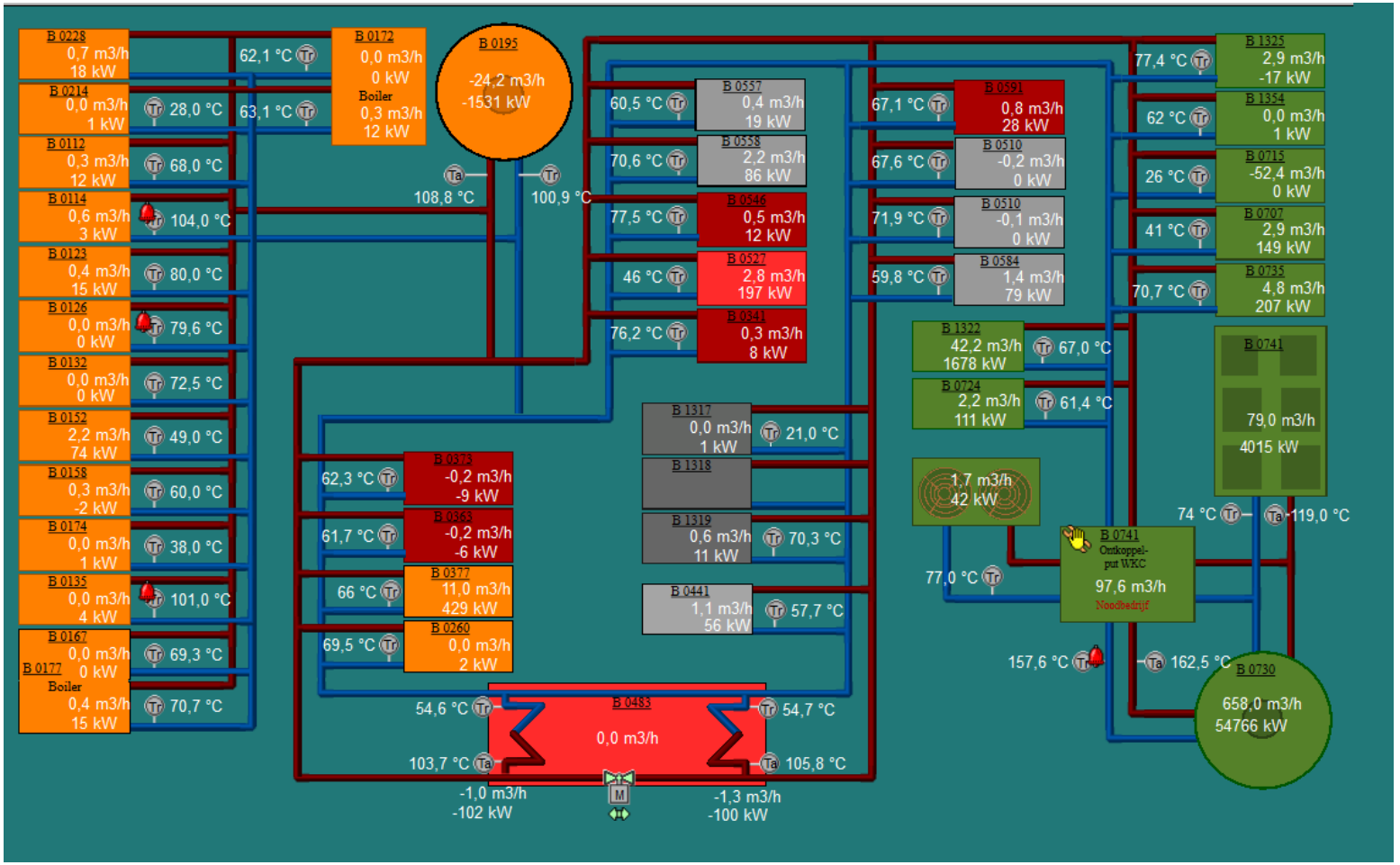

Figure A.2: Schematic presentation of the buildings connected to UU's own heat network.

A.3.2 ATES connections

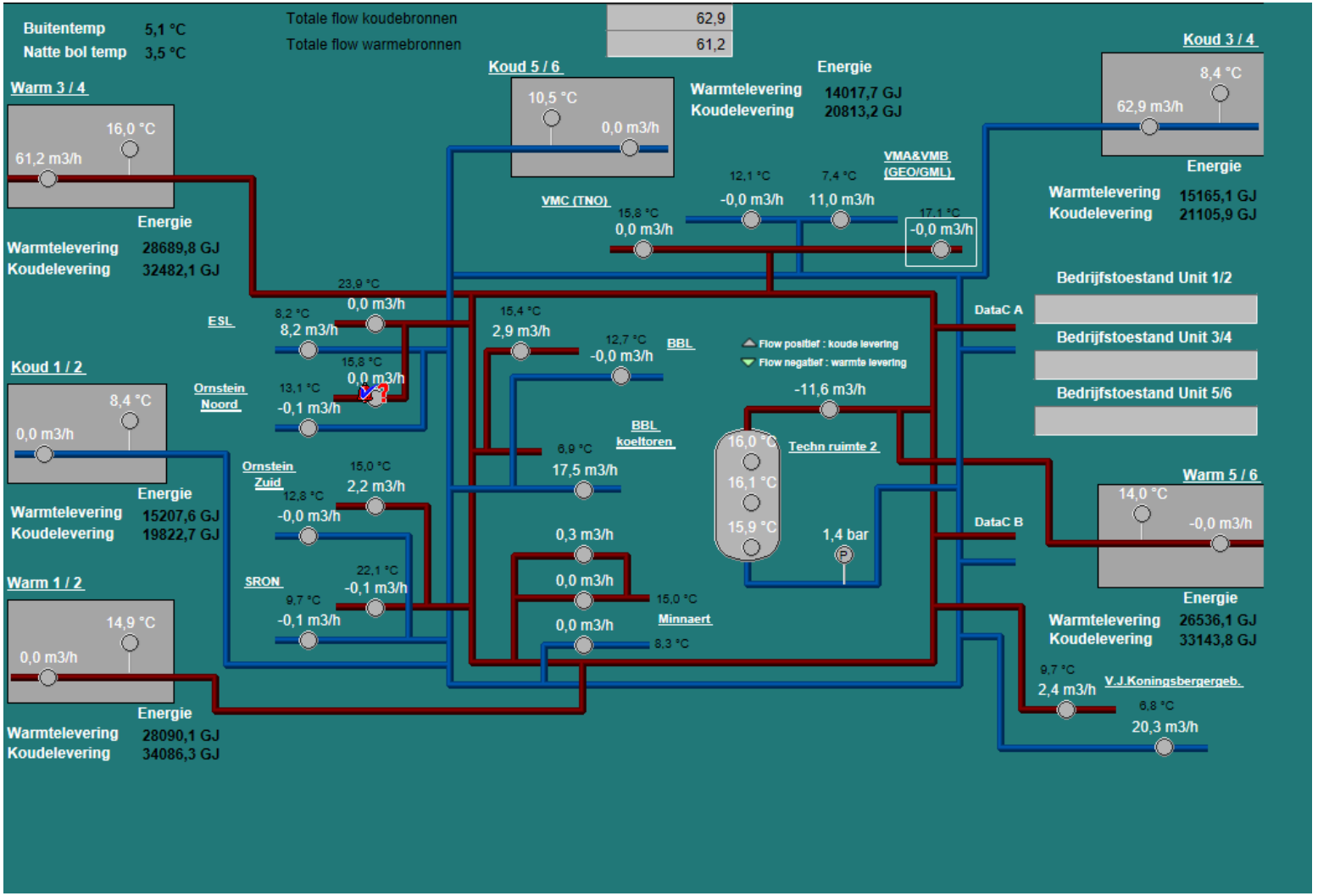

Figure A.3: Schematic presentation of the buildings connected to the existing ATES system in north west campus.

Appendix B

Technologies

B.1 Input data for conversion and storage technologies

Table B.1: Input data for conversion and storage technologies in the E-Hub. In this case α represents the energy coefficient 1, β energy coefficient 2, γ energy coefficient 3, δ the size coefficient 1, ζ size coefficient 2, κ size coefficient 3, ν size coefficient 4 and ρ the first principle to electrical efficiency ratio. For storage technologies η represents the conversion or storage efficiency, Λ the time variation, Φ the storage loss coefficient, τ the storage charging/discharging time, Θ^{min} the minimum air temperature, Θ^{max} the maximum air temperature and p the pressure

Conversion technologies	α	β	$\gamma[kW]$	δ	$\zeta[kW]$	κ	$\nu[kW]$	ρ
boiler	0.92							
edHP	3.59	−0.08	0.10	0.13	0.01	0.99	0.01	
PEMEC	{0.60, 0.55, 0.53, 0.51}	{−0.01, 0.02, 0.01, 0.03}	0	0.07	0	1	0	
PEMFC H_2	{0.59, 0.54, 0.50, 0.47}	{−0.00, 0.02, 0.06, 0.11}	0	0.01	0	1	0	1.71
Storage technologies	η	$\Lambda[h^-1]$	Φ	$\tau[hr]$	Θ^{min} [°C]	Θ^{max} [°C]	p $[bar]$	
HOS	1	0	0	4			40	
HWTS	0.90	0.005	0.001	4	65	90	1.01	
LiB	0.93	0.001	0	3				

B.2 Cost coefficients of conversion and storage technologies.

Table B.2: Cost coefficients of conversion and storage technologies implemented in the E-Hub. In this case θ represents the cost coefficient 1, μ cost coefficient 2, S^{min} the minimum technology size, S^{max} the maximum technology size and ψ the fraction for maintenance costs

Technology	θ	μ	S^{min}	S^{max}	ψ
boiler	{194.1; 82.4; 65.2} EUR kW^{-1}	{0; 6.88; 10.40} $\cdot 10^3$	{0.02; 0.07; 0.20}$\cdot 10^3$ kW	{0.07; 0.2; 2000} $\cdot 10^3$ kW	0.02
edHP	{2088.2; 1221.2; 930.9} EUR kW^{-1}	{0; 4.33; 13,0} $\cdot 10^4$	{0.02; 0.05; 300}$\cdot 10^3$ kW	{0.05; 0.3; 2000}$\cdot 10^3$ kW	0.015
HOS	{20.7; 13.6; 10.9} EUR kWh^{-1}	{0; 0.24; 9.45} $\cdot 10^3$	{0; 0.03; 3.33} $\cdot 10^3$ kWh	{0.033; 3.33; 4929} $\cdot 10^3$ kWh	0.03
HWTS	{10.5; 7.5; 6.25} EUR kWh^{-1}	{0; 8.4; 22.9} $\cdot 10^4$	{0; 0.28; 0.3} $\cdot 10^4$ kWh	{0.28; 0.3; 400} $\cdot 10^4$ kWh	0.02
LiB	500 EUR kWh^{-1}	-	0 kWh	50 $\cdot 10^6$ kWh	0.04
PEMEC	{2693; 1727; 1354} EUR kW^{-1}	{0; 9.67; 24.6}$\cdot 10^4$	{0; 0.1; 0.4}$\cdot 10^2$ kW	{0.1; 0.4; 1000}$\cdot 10^3$ kW	0.05
PEMFC H_2	{2160; 1680; 1320} EUR kW^{-1}	{0; 3.2; 8.0}$\cdot 10^5$	{0; 0.50; 1.33}$\cdot 10^3$ kW	{0.50; 1.33; 1000}$\cdot 10^3$ kW	0.08
PV	375 EUR m^{-2}		0 m^2	1 289 014 m^2	0.04
ST	500 EUR m^{-2}		0 m^2	1 289 014 m^2	0.04
WT 1500	2.10 mEUR $unit^{-1}$				0.04
WT 2500	3.13 mEUR $unit^{-1}$				0.04
WT 4500	4.95 mEUR $unit^{-1}$				0.04